Available online at www.sciencedirect.com
ScienceDirect
Continental Shelf Research 28 (2008) 2071–2091
CONTINENTAL SHELF RESEARCH
www.elsevier.com/locate/csr

Impact of natural (waves and currents) and anthropogenic (trawl) resuspension on the export of particulate matter to the open ocean Application to the Gulf of Lion (NW Mediterranean)

B. Ferré[a], X. Durrieu de Madron[a,*], C. Estournel[b], C. Ulses[b], G. Le Corre[c]

[a]*CEFREM, CNRS—Université de Perpignan, Perpignan, France*
[b]*LA, CNRS—Université de Toulouse, Toulouse, France*
[c]*IFREMER, DRH, Sète, France*

Received 20 March 2007; received in revised form 4 February 2008; accepted 9 February 2008
Available online 17 February 2008

Abstract

Modern sediment deposits on continental margins form a vast reservoir of particulate matter that is regularly affected by resuspension processes. Resuspension by bottom trawling on shelves with strong fishing activity can modify the scale of natural disturbance by waves and currents. Recent field data show that the impact of bottom trawls on fine sediment resuspension per unit surface is comparable with that of the largest storms.

We assessed the impact of both natural and anthropogenic processes on the dispersal of riverborne particles and shelf sediments on the Gulf of Lion shelf. We performed realistic numerical simulations of resuspension and transport forced by currents and waves or by a fleet of bottom trawlers. Simulations were conducted for a 16-month period (January 1998–April 1999) to characterise the seasonal variability. The sediment dynamics takes into account bed armoring, ripple geometry and the cohesive and non-cohesive characteristics of the sediments. Essential but uncertain parameters (clay content, erosion fluxes and critical shear stress for cohesive sediment) were set with existing data. Resuspension by waves and currents was controlled by shear stress, whereas resuspension by trawls was controlled by density and distribution of the bottom trawler fleet.

Natural resuspension by waves and currents mostly occurred during short seasonal episodes, and was concentrated on the inner shelf. Trawling-induced resuspension, in contrast, occurred regularly throughout the year and was concentrated on the outer shelf. The total annual erosion by trawls (5.6×10^6 t y^{-1}, t for metric tonnes) was four orders of magnitude lower than the erosion induced by waves and currents (35.3×10^9 t y^{-1}). However the net resuspension (erosion/deposition budget) for trawling (0.4×10^6 t y^{-1}) was only one order of magnitude lower than that for waves and currents (9.2×10^6 t y^{-1}).

Off-shelf export concerned the finest fraction of the sediment (clays and fine silts) and took place primarily at the southwestern end of the Gulf. Off-shelf transport was favoured during the winter 1999 by a very intense episode of dense shelf water cascading. Export of sediment resuspended by trawls (0.4×10^6 t y^{-1}) was one order of magnitude lower than export associated with natural resuspension (8.5×10^6 t y^{-1}). Trawling-induced resuspension is thought to represent one-third of the total export of suspended sediment from the shelf.

A simulation combining both resuspension processes reveals no significant changes in resuspension and export rates compared with the sum of each individual process, suggesting the absence of interference between both processes.

Keywords: Sediment dynamics; Sediment transport; Shelf–slope exchanges; Fisheries; Trawling; Mediterranean

1. Introduction

Continental margins are located at the edges of continents and form a buffer zone where the oceans, continents and atmosphere interact. Significant quantities

*Corresponding author. Tel.: +33 4 68 66 22 48; fax: +33 4 68 66 20 96.
E-mail address: demadron@univ-perp.fr (X. Durrieu de Madron).

0278-4343/$ - see front matter © 2008 Elsevier Ltd. All rights reserved.
doi:10.1016/j.csr.2008.02.002

of organic and inorganic material are input to continental margins where intense hydrodynamic conditions control their dispersal on the shelf and towards the open sea. The sedimentary compartment on continental margins appears to be a vast reservoir of particulate matter, in particular river-derived material, and also of dissolved constituents. Resuspension of sediment causes a significant redistribution of sediments and has important implications for regional particulate matter budgets and export to deeper environments, i.e., the continental slope and rise.

Nowadays the physical resuspension and disturbance of sediment on continental shelves is a combination of both natural and anthropogenic mechanisms. Waves and currents are the major initiators of natural disturbance that can result in potentially massive sediment redistribution. The large-scale disturbance they induce can be periodic, when associated with tidal currents, or episodic, when associated with storms. On the other hand, commercial bottom trawling has a more reduced and patchy footprint. Bottom fishing gear (trawl, dredge) efficiently scrapes the superficial sediment and generate suspended sediment plumes. In many shelves fishing intensity is high and most fishable grounds, which can extend to 1000 m in depth, are likely to be disturbed more or less frequently. The effect of sediment resuspension by waves and currents and bottom trawling is site-specific, as it depends on hydrodynamic conditions (storm frequency and intensity, tidal motions), sediment characteristics (grain size, cohesiveness) and fishing activity (frequency and geographical distribution of bottom hauls, gear type).

The relative contribution of each mechanism to the resuspension and export of sediment on continental shelves has seldom been addressed. To our knowledge, Churchill (1989) and DeAlteris et al. (1999) carried out the only preliminary studies on the comparison of the effect of natural and anthropogenic resuspension on different areas of the Mid-Atlantic Bight (Narraganset Bay, Nantucket Shoals and Virginia Shelf). These studies concluded that natural physical processes denote the primary suspension mechanism in shallow environments, where they disturb the bed regularly, while trawling appears to be the primary resuspension mechanism in deeper environments where natural processes are weaker and rarely capable of eroding sediment. Furthermore, Churchill (1989) estimated, using current meter data and simple analytical models, that transport of sediment resuspended by trawlers on muddy regions of the outer shelf could contribute to the off-shelf transport of particulate matter.

The present paper aims to assess the impact of sediment resuspension on particulate matter budgets on the Gulf of Lion continental shelf (NW Mediterranean). It discriminates the impact of natural physical (waves and currents) and anthropogenic (bottom trawling) processes, and thereby evaluates whether anthropogenic disturbance represents a significant or just a slight modification in the scale of existing natural disturbance. This work uses three-dimensional numerical models coupling the hydrodynamics with the sediment dynamics associated with waves and currents and/or trawling. The parameterisations used in the models are based on experimental studies of the resuspension of fine sediments by intense storms (Ferré et al., 2005; Ulses et al., this issue) and trawls (Durrieu de Madron et al., 2005). Simulations over one annual period, using realistic forcing, were carried out to characterise and quantify (i) the temporal variability and magnitude of sediment resuspension on the shelf, (ii) the dispersal of resuspended sediment and (iii) the export towards the open sea.

The outline of this paper is as follows: the regional setting is described in Section 2, the hydrodynamical and sediment transport models are briefly described in Section 3, the numerical simulations of sediment resuspension and export are exposed in Section 4, comparison of resuspension processes and their impact of the sediment budgets are presented in Section 5, a summary is given in Section 6, and the model equations are given in the appendix.

2. Regional setting

2.1. Physiography and hydrodynamics

The Gulf of Lion is a non-tidal and river-dominated margin in the northwestern Mediterranean (Fig. 1a). It is fed by 10 rivers, one of them being the Rhône, which is the major Mediterranean river. Its crescent shape and the circulation patterns favour off-shelf export of particulate matter at the southwestern end of the Gulf (Monaco et al., 1999; Heussner et al., 2006; Palanques et al., 2006).

The median grain size of superficial bottom sediments is shown in Fig. 1b. Sands of the inner shelf display a seaward-fining texture and merge with mid-shelf muds in water deeper than 20–30 m. The only noticeable exception is the prodeltaic accumulation zones found near river mouths, which are composed of silty muds. Muddy deposits on the outer shelf (>90 m) are mixed with relict sandy outcrops.

The different wind regimes determine the natural resuspension and transport of suspended sediment on the shelf. Predominant N–NW winds generally induce distinctive and opposing circulation cells on the shelf, favouring intrusion of slope waters in the eastern and central parts, and export of shelf water at the southwestern end of the Gulf (Estournel et al., 2003; Petrenko et al., 2004; Ulses et al., 2008). Furthermore, these cold and dry continental winds are responsible for the strong cooling and homogenisation of the shelf water column during winter, and eventually generate dense water (Dufau-Julliand et al., 2004; Ulses et al., 2008). Due to the reduced fetch, N–NW winds generate small waves (significant wave height <2 m, peak period <6 s) on the inner shelf. Episodic and short-lived E–SE winds induce a sea level rise at the shore and an overall intense cyclonic circulation on the shelf (Ulses et al., 2008). These winds are associated with a long fetch and large swell (significant wave height up to 10 m, peak period up to 12 s). River floods often occur

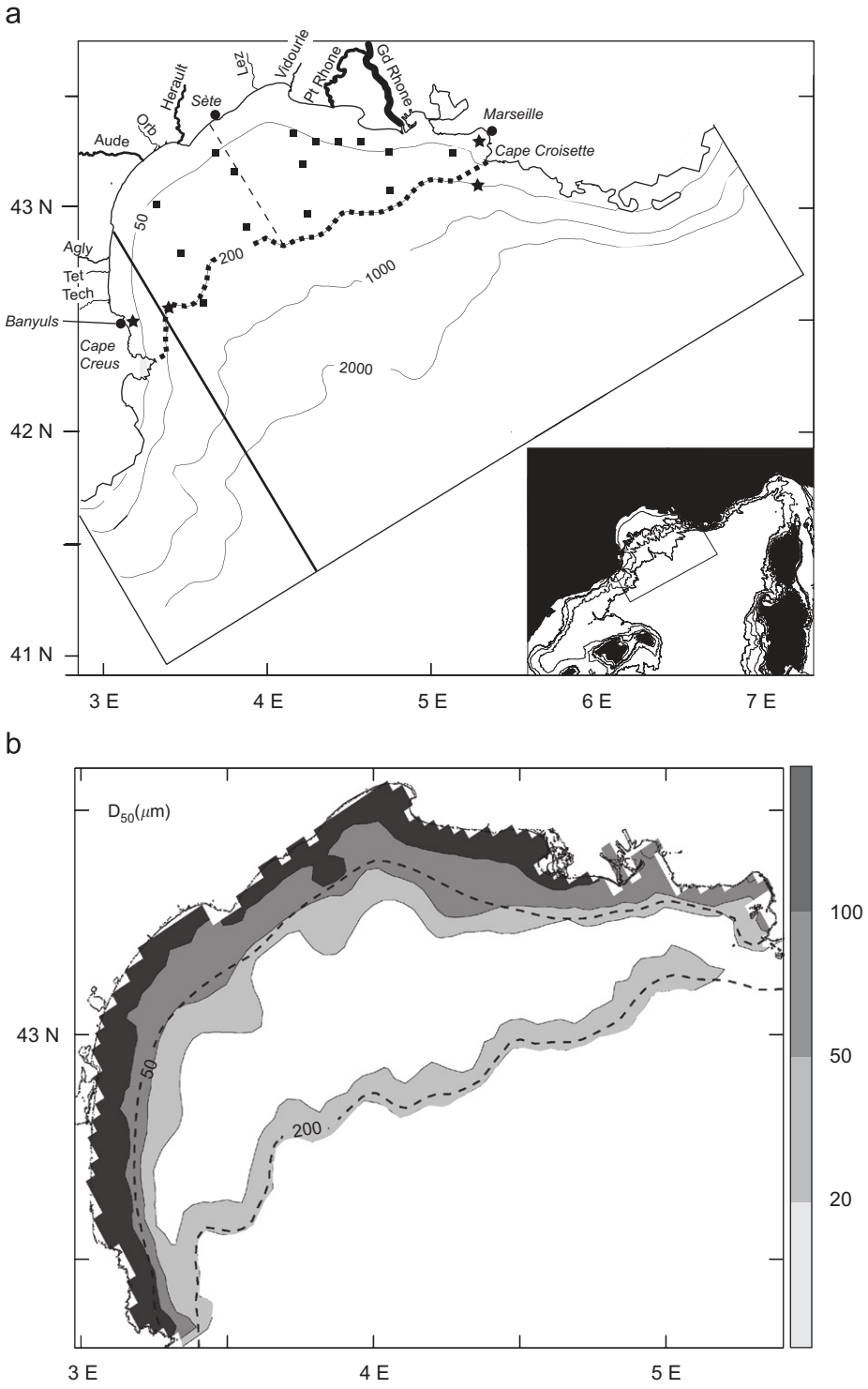

Fig. 1. (a) Bathymetry of the Gulf of Lion in the model and position of hydrological stations. The thick dashed line around the shelf break depth (200 m) between Cape Croisette and Cape Creus delineates the limit between the shelf and the open sea. Stars near the coast and within canyon heads represent the location of the bottom-shear stress estimates (Fig. 3e) and near-bottom density anomaly estimates (Fig. 3f). The shelf is subdivided in two halves (cross shelf thin dashed line) for water flux estimates given in Fig. 3g. (b) Median grain size of superficial sediment showing the seaward-fining texture of the sediment and coarsening around the shelf edge.

in conjunction with E–SE storms as the transport of humid marine air over coastal relief induces abundant precipitation. Resuspension by natural physical processes results primarily from the effect of southeasterly swells associated with E–SE winds (Ferré et al., 2005; Guillén et al., 2006).

A permanent cyclonic current (the Northern Current) flows along the slope and is part of the general circulation

of the western Mediterranean basin (Millot, 1999). It forms a density front that separates the low-salinity shelf water from the more saline open sea water, limiting the off-shelf dispersal while enhancing along-slope dispersal (Durrieu de Madron et al., 1990; Lapouyade and Durrieu de Madron, 2001). Hence, constrained by the slope current offshore and the coast inshore, most shelf water and suspended sediments are funneled towards the narrowing south-western shelf end. They are advected out of Gulf of Lion's shelf, by flowing alongshore around the Cape Creus promontory or down the nearby canyons.

2.2. Characteristics of trawling activity

About 128 trawlers coming from the local fishing ports (Port-Vendres, Port-la-Nouvelle, Agde, Sète, Grau du Roi, Port de Bouc) are working in the Gulf of Lion, using either semi-pelagic or bottom trawls to catch demersal fish species. Bottom trawlers use single trawl nets tightened between doors (otter) with a tickler chain as a groundrope. Pelagic trawls are sometimes also used very near the seabed, but Durrieu de Madron et al. (2005) showed that they had no impact on the sediment resuspension. The daily number of trawlers using bottom trawls ranges approximately between 40 and 90 boats, each trawler performing four to five tows of about 2 h daily. They work throughout the year except weekends and public holidays.

Fishing grounds cover the whole continental shelf except for a 3-mile coastal band, where all trawling activity is banned. A survey conducted with fishermen revealed that the wind is the principal criterion for the choice of the fishing grounds. Trawlers remain basically close to the coast during strong winds ($>10\,m\,s^{-1}$ or 20 knots) and rough seas state periods, and move to the outer shelf for weaker winds and calmer sea state.

3. Material and methods

3.1. Hydrodynamical model

3.1.1. The SYMPHONIE model

The three-dimensional primitive equation coastal ocean model SYMPHONIE (Marsaleix et al., 2008), used in this study, has been extensively validated in the Gulf of Lion. It was previously used to study the Rhône river plume (Estournel et al., 1997, 2001; Marsaleix et al., 1998), the intrusion of the Northern Current into the shelf (Petrenko et al., 2004), the wind-induced circulation (Estournel et al., 2003) and the formation of dense water on the shelf and its cascading over the slope (Dufau-Julliand et al., 2004; Ulses et al., 2008).

The horizontal and vertical components of the current, free surface elevation, temperature and salinity are computed on a C staggered-grid (Arakawa and Suarez, 1983). A generalised topography following coordinate system is used. Compared to a simple sigma coordinate, the generalised sigma coordinate allows the slope of the iso-level surface to be limited over steep topography in order to avoid large truncation errors on the pressure gradient computation (Auclair et al., 2000). The turbulence closure scheme is based on a prognostic equation for the turbulent kinetic energy and on a diagnostic equation for the mixing and dissipation length scales (Bougeault and Lacarrere, 1989). A leap frog scheme is used for the time-stepping. A time-splitting technique (Blumberg and Mellor, 1987) allows the vertical shear of the current and the depth-averaged horizontal components to be computed separately with appropriate time steps. The time step of the internal mode is set to 180 s.

3.1.2. Initialisation and boundary conditions

The domain of the Gulf of Lion model (25 vertical levels and 3 km horizontal resolution grid) is presented in Fig. 1a. The main boundary of the modelling domain has been chosen to be parallel to the continental slope.

At the surface, the momentum flux is equal to the wind stress. The heat flux results from the atmospheric fluxes (sensible and latent heat fluxes) and from the radiative fluxes (both short and long wavelengths); the salinity flux is calculated from evaporation. Concerning the turbulent kinetic energy, the usual boundary-layer balance between production and dissipation is applied. The wind stress and the heat fluxes are computed with the bulk formulae (Geernaert, 1990) using 6-h outputs of the high-resolution meteorological models ARPEGE and ALADIN from Météo-France (surface pressure, air temperature, relative humidity and wind velocity) and the sea surface temperature is computed by the ocean model.

At the sea floor, the near-bottom stress is related to the horizontal bottom velocity and waves, as well as the seabed roughness. A detailed description of this term is given in Appendix B. Heat and salinity fluxes are considered to be zero at this boundary. The turbulent kinetic energy is parameterised similarly to that at the top boundary.

At open lateral boundaries, the free-surface elevation (η) and the component of transport orthogonal to the boundary (U) are given by the radiation condition of Oey and Chen (1992): $U = U_0 \pm (gH)^{1/2}\,(\eta - \eta_0)$. Other variables are given by $\nabla_{H\varphi} = \nabla_H \varphi_0$, where φ stands for the tangential component of the depth-averaged current and baroclinic velocities. U_0, φ_0 and η_0 refer to the large-scale field forcing. Concerning temperature and salinity, an upstream condition implies that large-scale fields, $T_0(t)$ and $S_0(t)$, are advected into the simulated domain under inflow conditions. The large-scale fields are also applied over the whole grid at $t = t_0$ (initialisation). This initial state aims to start the simulation with the large-scale geostrophic circulation of the Gulf of Lion, generally identified as the Northern Current. The model is initialised with a fully established along-slope circulation adjusted to bathymetry constraints, based on a linearised derivation of the external mode equations of the model (Estournel et al., 2003). The regional model was initialised and forced every day by the large-scale Ocean General Circulation Model (OGCM)

MOM outputs. Wave characteristics over the domain were described by the 6-h outputs of the Vagmed waves-forecast model of Météo-France.

Concerning the buoyancy inputs, the freshwater inputs for the main rivers of the Gulf of Lion (Grand-Rhône, Petit-Rhône, Vidourle, Lez, Herault, Orb, Aude, Agly, Têt, Tech) (see Fig. 1a), are taken into account. Daily discharges provided by the "Compagnie Nationale du Rhône" and by the "Banque Hydro-MEDD/DE" were specified at the 10 river mouths. The temperature in all rivers is set following measurements in Rhône river (Poirel et al., 2001), with a maximum value of 22 °C in October and a minimum value of 7 °C in January and February.

3.2. Sediment transport model

The suspended sediment transport model aims at simulating the dispersal of the sedimentary particles resuspended by waves and currents, as well as bottom trawls. This model is governed by an advection-diffusion dispersion equation, and considers different particle grain sizes (see Appendix A). Deposition and erosion terms are incorporated into the seabed boundary condition. The erosion term was estimated with sediment dynamic models specific to each resuspension mechanisms (waves and current, trawls); they are described in the following chapters and in Appendix B.

Given that the Gulf of Lion sediments cover a wide range of sizes (Fig. 1b), primary (individual) particles in the sediment were clustered in seven size classes ranging from clay to coarse sand, according to the Wentworth classification (1922). Two additional classes were considered for suspended particles to take into account aggregated particles. The aggregate characteristics were inferred from comparisons between *in situ* and laboratory particle size distribution of resuspended sediment (Durrieu de Madron et al., 2005). These measurements suggested that about three-fourths of the clays and one-fourth of the fine silts are incorporated into aggregates whereas the rest remains as primary particles. We considered that clays and fine silts contributed equally to the formation of both classes of aggregates. The characteristics of each class (median grain size, settling velocity and density) are indicated in Table 1.

River sediment inputs were computed using water discharge (Q) and suspended sediment concentration estimates ($SSC = f(Q)$) established by different authors: Sempéré et al. (2000) for the Rhône River, Pethelet-Giraud et al. (2003) for the Hérault River, Serrat (1999) for the Agly River and Serrat et al. (2001) for the Têt River. In absence of information for Orb and Aude Rivers, we used the relationship of the nearby Hérault River. Finally, solid discharge of the Rhône River was divided into two parts: 90% for the Grand-Rhône branch and 10% for the Petit-Rhône branch. Grain size distribution of river inputs was defined according to recent data collected in the Rhône River (Radakovitch, personal communication) and Têt River (Garcia-Estevez, 2005). All "small" rivers (Hérault, Agly, Orb, Aude, Vidourle and Tech) are considered to have the same grain distribution as the Têt River. Most of the suspended particles are silts (ca. 80% for the Rhône River and 69% for the Têt River) and clays (~18% for the Rhône River and 24% for the Têt River). The sediment provided by the rivers is homogeneously input in one mesh, and settles and/or is transported as it enters the domain.

The grain size distribution of the shelf surface sediments was determined from the compilation of several sedimentological surveys that provided about 160 cores over the whole shelf. Fig. 1b shows the median grain size of the first centimetres of the sediment. Maps of the fraction of the different size classes were used at the initial time. Their characteristics slightly changed throughout the simulation according to the dispersal of river inputs, and the erosion and deposition of the different classes of sediment.

3.3. Sediment dynamics for waves and currents

Sediment erodability is controlled by the shear stress intensity and the bottom sediment properties (coarse non-cohesive vs. fine cohesive sediments). The limit between cohesive and non-cohesive sediment was fixed at 10% of clay ($<4\,\mu m$), which is in the range (3–14%) defined in various studies (Dyer, 1986; Torfs, 1995; Panagiotopoulos et al., 1997; Houwing, 2000). The Partheniades' law (1962) was used to compute the erosion flux of cohesive sediments, whereas the reference concentration based on the method of Zyserman and Fredsøe (1994) was used for the erosion flux of the non-cohesive sediments (see Appendix B).

Bottom-shear stresses were computed using combined wave and current conditions, and discriminated flat-bed and rippled bed conditions (see Appendix B). The bottom roughness calculation and ripple geometry for the non-cohesive sediments were based on the SEDTRANS96 model (Li and Amos, 1998, 2001), which predicts the roughness and bedforms generated by a combined wave/current model. For cohesive and mixed sediments, the

Table 1
Characteristics of particle grain size classes used in the sediment transport model

Class	1	2	3	4	5	6	7	8	9
Category	Clay	Fine silt	Coarse silt	Very fine sand	Fine sand	Median sand	Coarse sand	Aggregates	
D_{50} (μm)	2.43	8.39	31.6	92.4	179.21	317	1063	31.6	129.5
W_s ($m\,s^{-1}$)	4.6×10^{-6}	5.5×10^{-5}	7.7×10^{-4}	6.6×10^{-3}	2.0×10^{-2}	4.1×10^{-2}	1.6×10^{-1}	1.1×10^{-4}	5.9×10^{-4}
ρ ($kg\,m^{-3}$)	2650	2650	2650	2650	2650	2650	2650	1264	1097

roughness scale model of Harris and Wiberg (2001) was used. Bed armoring was also implemented in the model to take into account the reduction of erosion flux of fine particles in mixed sediments, due to the protective effect of larger sand grains (Harris and Wiberg, 2001).

The critical shear stress (stress above which the sediment is likely to be removed) depends on grain size and sediment characteristics. For non-cohesive sediments, the critical shear stress is given in the form of a critical shields parameter value, which depends on the grain size of each class (see Appendix B). For cohesive sediments, the threshold value is difficult to establish because it depends on the compaction and history of the sediment. Indeed, an unconsolidated surface layer (fluff) is eroded for very weak shear stresses, ranging between 0.02 and 0.08 $N\,m^{-2}$ (El Ganaoui et al., 2004; Gust and Morris, 1989; Maa et al., 1998; Schaaff et al., 2002). The underlying, more consolidated layers, need larger critical shear stresses, between 0.1 and 0.61 $N\,m^{-2}$ (Maa et al., 1998; Houwing, 1999; Krishnappan and Marsalek, 2002; Palanques et al., 2002). In this study the model does not include a fluff layer, and an average critical shear stress of 0.2 $N\,m^{-2}$ is given for all of the cohesive sediment.

3.4. Resuspension by bottom trawls

In absence of direct information about the distribution and movement of trawlers on the shelf (such as those provided by Vessel Monitoring System), we used a probabilistic approach and the fishing rules in force in the area to simulate their daily position and trajectory. Based on sample surveys of the fisherman population of the different ports about its preferential fishing grounds and depths, we derived an average trawling activity within a daily operating range from each port. These fishing patterns were generalised to the trawling fleet of each port, and the total fishing intensity in every locations of the shelf was derived by summing the effect of all fleets. The scores assigned to each location of the shelf area were finally used to weight partition the total fishing effort (Fig. 2). A distribution of fishing effort was simulated for wind speeds lower and larger than 10 $m\,s^{-1}$; the sea state being determinant for the choice of fishing grounds. The daily working time and number of active bottom trawlers were estimated from records of trawler fleets coming from the different fishing ports (Fig. 3d). During working days (i.e., apart from weekends and public holidays), each trawler was assumed to perform four tows of 2 h from 4 to 12 a.m.

The distribution map for each working day was selected according to the wind intensity next to the Sète port (major fishing port of the area) at 4 a.m. After being positioned randomly, each trawl was displaced using a random walk approach. Given the mesh size of the model (3 km) and the trawling speed (1.5 $m\,s^{-1}$), a crossing time of 33 min was considered before moving each trawler to one of the surrounding mesh. After this time, the eight surrounding cells have the same probability to be trawled. A maximum

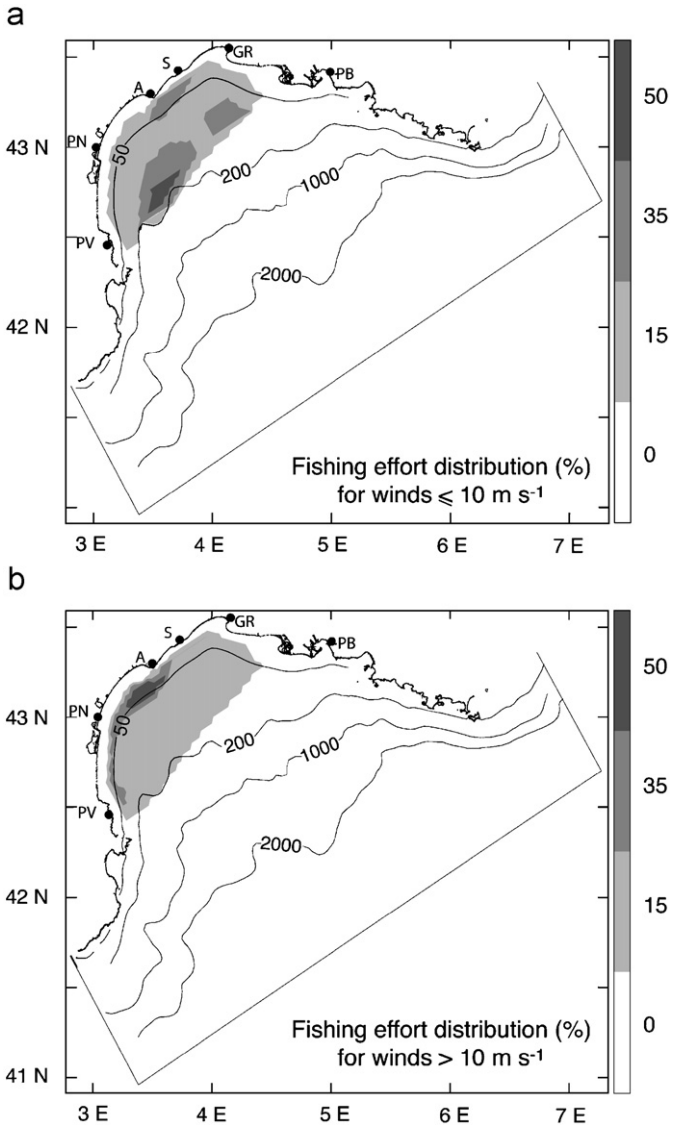

Fig. 2. Probability density distribution of bottom trawls for (a) weak wind ($\leqslant 10\,m\,s^{-1}$) and (b) strong winds ($>10\,m\,s^{-1}$). Black dots indicate the position of fishing ports sheltering the fleet of bottom trawlers: PV, Port-Vendres; PN, Port-la-Nouvelle; A, Agde; S, Sète; GR, Grau du Roi; PB, Port de Bouc. Isobaths 50, 200, 1000 and 2000 m superimposed as black lines.

number of three trawlers per mesh was imposed, to take into account interaction among fishing vessels. Albeit schematic, the simulated spatial allocations are believed to correctly reproduced the distribution of bottom trawling effort and displacement of vessels, but probably underestimate trawling activity in banned areas (e.g., within the 3-miles coastal band).

The fluxes of sediment resuspended by otter bottom trawls and the characteristics of the sediment plumes were estimated experimentally and described by Durrieu de Madron et al. (2005). They showed that resuspension fluxes depend on the trawl's groundrope gear, but above all, on sediment texture, i.e., fluxes increase with increasing clay content. Based on the measurements performed by Durrieu

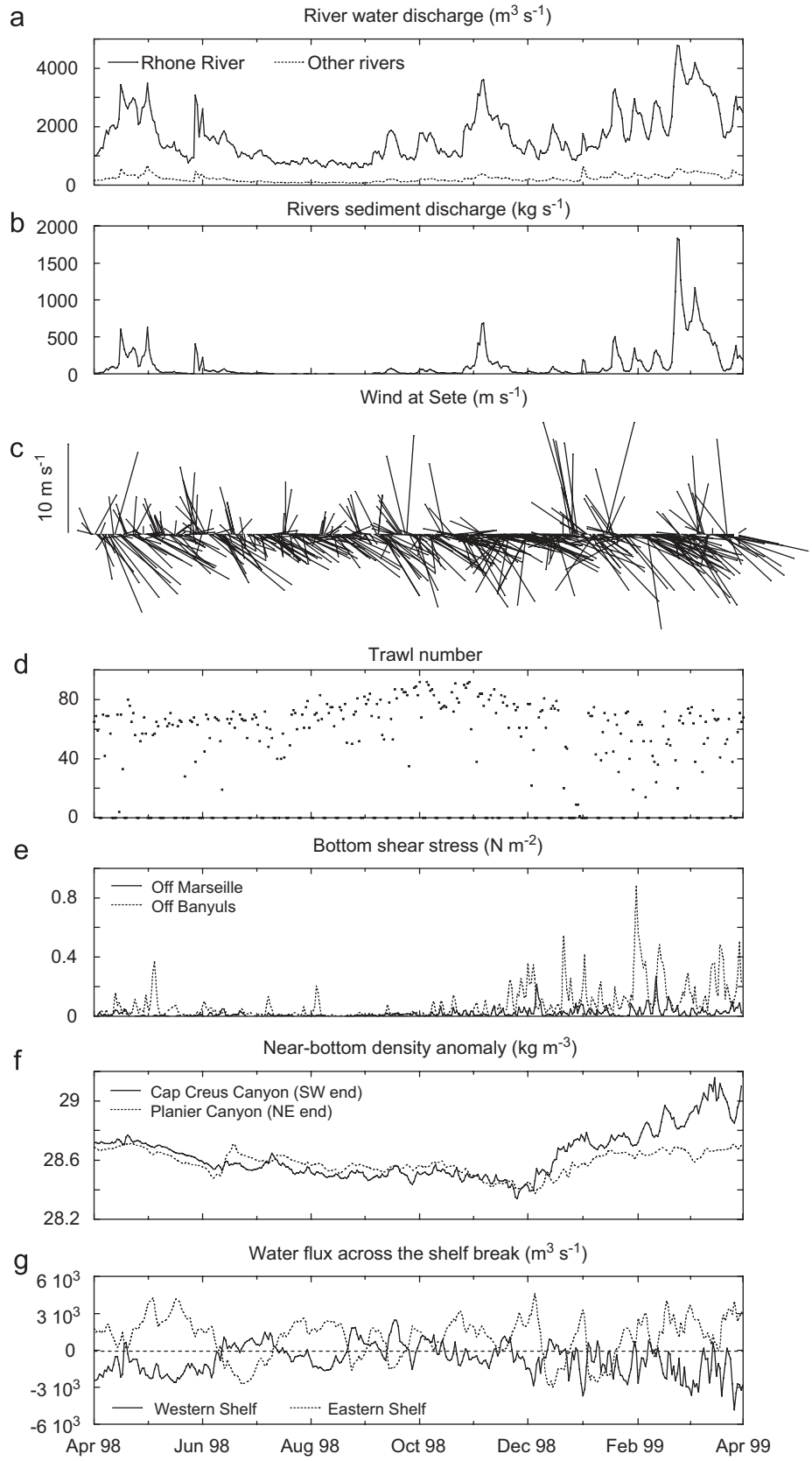

Fig. 3. Time series from April 1998 to April 1999 of (a) water discharge from the Rhône River and other rivers of the Gulf of Lion, (b) solid discharge from all rivers, (c) wind off Sète, (d) daily strength of bottom trawls in the Gulf of Lion, (e) bottom-shear stress off Marseille and Banyuls (see Fig. 1 for position), (f) water density anomaly at 200 m depth at the eastern end (Planier Canyon) and southwestern end (Cape Creus Canyon) of the Gulf and (g) and water flux across the shelf break (slope water import onto the shelf is positive, whereas shelf water export is negative).

de Madron et al. (2005), a linear relationship was derived between the resuspension flux and the clay fraction (see Appendix B). According to observations, resuspended sediment was distributed over the lowest 5 m above the seabed with a concentration inversely proportional to the seabed distance. For each time step (180 s), the resuspended mass of sediment in the model is calculated according to the clay fraction and is proportional to the trawled area: 4320 m^2 considering a trawler speed of 1.5 $m\,s^{-1}$ and a combined net and door width of 16 m. Because this area is much smaller than that of the model mesh (9 km^2), the resuspended mass was spread over the entire mesh and within layers including the lowest 5 m above bottom. The bias introduced by the forced diffusion is likely to be small, since most of the resuspended sediment is rapidly deposited (within 1–2 h according to Durrieu de Madron et al., 2005), and remains confined to the adjacent meshes.

3.5. Scenarios and numerical solutions

Four scenarios were carried out in order to answer the question about the role of resuspension in the shelf–slope exchanges of particulate matter. They considered the same hydrodynamic forcing conditions described in Section 3.1:

- The first simulation, which only takes into account the river particulate inputs (i.e., resuspension is absent), was used as reference for the shelf deposit and the export of riverine particulate matter for the study period.
- The second scenario considered, in addition to the preceding simulation, resuspension of sediment by currents and waves only.
- The third scenario considered sediment resuspension by trawls only.
- A fourth scenario combining resuspension by waves and currents, as well as trawls, checked if there is any significant nonlinear effect.

Simulations lasted 16 months from January 1, 1998 to April 1, 1999. The water column was clear of suspended particles at the initial time, and the system was gradually loaded in suspended particles, coming from rivers and/or sediment resuspension during the first months of simulations. As the residence time of shelf waters is about 2 months (Durrieu de Madron et al., 2003), we checked that the suspended sediment concentration (SSC) of the shelf water was stabilised on the third month (March 1998). For each scenario, annual budgets of resuspended sediment, deposited particles on the shelf, and exported particles to the slope, were calculated between April 1998 and April 1999. The shelf-edge for these calculations is defined as the 200-m isobath between Cape Creus and Cape Croisette (cf. Fig. 1a for the boundary). Sediment export from the Gulf of Lion's shelf is calculated by accumulating at each time step the difference between resuspension and deposition on the shelf and then by subtracting the sediment present in the water column and delivered by rivers.

Hydrography and circulation on the shelf and upper slope were measured during two surveys conducted in March/April 1998 and January 1999. Previous studies tested the ability of the hydrodynamical model to correctly reproduce the hydrography and wind-induced circulation patterns observed in March/April 1998 (Estournel et al., 2003), and the formation of dense water on the shelf and its cascading over the slope in January/February 1999 (Dufau-Julliand et al., 2004). Critical but indefinite parameters of the sediment dynamics model (i.e., clay content threshold for cohesive/non-cohesive behaviour, erosion flux and critical shear stress for cohesive sediments) were adjusted to fit the in situ observations collected all over the shelf during these surveys. Parameters were chosen in order to have the smallest relative error ($|SSC_{in\ situ}-SSC_{model}|/SSC_{in\ situ}$), keeping in mind that measured concentrations include other sources of particulate matter (atmosphere, rivers, biology or advection onto the domain) which are not taken into account in the model. For these reasons, stations near the Rhône river mouth, near the slope or outside of the shelf are not used because they are likely to contain a majority of particles which are not from resuspension. The location of the casts used for comparison is shown in Fig. 1a. The agreement was quantified by computing the relative error between simulated SSC values (combining both resuspension by waves and current conditions and trawling activity) within the lowest three levels above the bottom with observed near-bottom SSC, estimated from optical (light transmission) measurements. This comparison is possible because of a weak fluorescence during the surveys (corresponding to near-bottom chlorophyll-*a* concentration $<0.2\,\mu g\,L^{-1}$), indicating a negligible biological fraction. Extreme parameters from the literature were first tested and the adjusted parameters yielded a relative error in SSC less than 35% for more than half of the stations and maximum differences of 80%.

4. Results

4.1. Hydrodynamical conditions

During the simulation period (April 1998–April 1999) the Rhône River supplied, respectively, 80% of the freshwater and 90% of the suspended sediment inputs to the Gulf (Fig. 3a,b). The annual total solid discharge, amounting to 3.6×10^6 t (metric tonnes), was supplied during moderate floods occurring mostly during spring 1998 and late autumn 1998–winter 1999 (Fig. 3b). Given that the average sediment discharge from the Rhône over the 1977–2004 period is about $10.1\times10^6\,t\,y^{-1}$ with extreme peaks at more than $33\times10^6\,t\,y^{-1}$ (Bourrin and Durrieu de Madron, 2006), the 1998–1999 period appears as a low discharge year.

E–SE gales were rare and brief but caused locally strong precipitations and sudden floods. N–NE continental winds were predominant throughout the year (Fig. 3c). These cold and dry winds affected the annual cycle of the shelf water thermal characteristics, by inducing strong mixing

and cooling during fall and winter. As the average salinity of the shelf water was rather constant over the year, decreasing temperature induced a progressive increase of density that culminated in late winter (Fig. 3f). During winter 1999, dense shelf water overflowed the shelf break and cascaded down the slope. Export of water mainly occurred in the western part of the shelf, and was compensated by an inflow in the eastern part of the Gulf (Fig. 3g). Béthoux et al. (2002) showed that an event of such intensity had not occurred since 1993, and that the last event probably went back to the winters 1987–1988. An event of similar intensity was observed in winter 2005 (Canals et al., 2006).

Bottom stress displays a seasonal cycle with larger values between the end of autumn and the beginning of spring (Fig. 3e), due to an increase in current intensity and wave conditions, and also to the weak stratification or even vertical homogeneity of the shelf water. Wind intensity and direction variability induced many bursts in the bottom stress, which was generally more intense on the western part of the shelf.

In summary, the study period was characterised by low river discharges and moderate wave conditions (with few E–SE storms), but by intense winter shelf water export through dense water cascading caused by sustained N–NW winds.

4.2. Fate of river inputs without resuspension

A first simulation was carried out by taking into account the sediment supplied by rivers only, in order to estimate the direct contribution of rivers to the sediment export (Fig. 4). During the April 1998–April 1999 period 3.6×10^6 t of sediment were discharged by rivers (Table 2). As previously mentioned, most input derived from the Rhône River. Deposits of river sediment on the shelf, which amounted to 3.1×10^6 t, clearly reflected the difference in river discharges (Fig. 3a). Sediments supplied by the Hérault, Orb and Aude Rivers in the northwestern part of the Gulf remained primarily confined to the inner shelf. Deposit of the Rhône River inputs formed a wedge extending over the eastern part of the shelf and the outer shelf as far as the southwestern end of the Gulf. The net deposit thickness was larger near the major river mouth, and was about 0.1 mm on most of the shelf. The grain size distribution reflected the accumulation gradient, with an early settling of the coarser particles on the prodeltas, and a fining texture along the transport pathways. Sediments in suspension exported from the shelf were mainly composed of fine particles. The exported quantity was 0.4×10^6 t (only 11% of river inputs (Table 2 and Fig. 5) and two-thirds of the export occurred during the wintertime (December 1998–April 1999).

4.3. Dynamics of resuspended sediments

4.3.1. Resuspension and off-shelf sediment export induced by waves and currents

Time series of the daily mass of sediment resuspended on the shelf (Fig. 6a) showed that resuspension by waves and currents appeared as short events, with a maximum

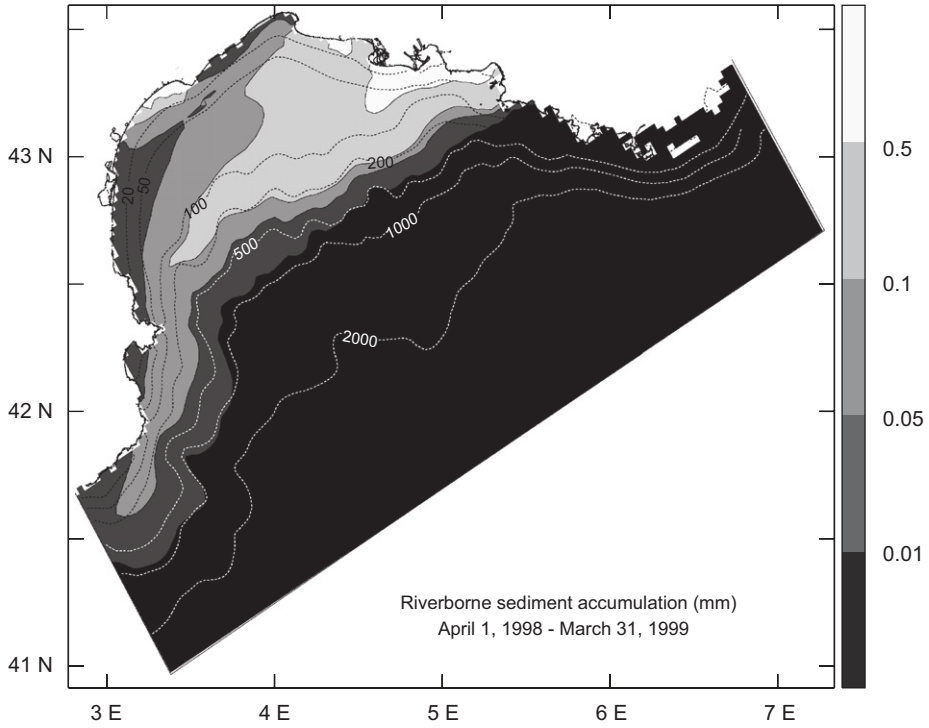

Fig. 4. Map of sediment thickness accumulated between April 1, 1998 and March 31, 1999 taking solely into account sediment discharges from rivers (no resuspension allowed).

Table 2
Annual sediment fluxes (in million metric tonnes per year) integrated between April 1, 1998 and March 31, 1999

Sediment fluxes	Scenario				
	Rivers	Storms	Trawling	Sum (storms + trawling)	Mixed (storms and trawling)
River discharge (10^6 t y^{-1})	3.57	3.57	3.57	3.57	3.57
Shelf erosion (10^6 t y^{-1})	0	35264.61	5.55	35270.16	35209.43
Shelf deposition (10^6 t y^{-1})	3.05	35255.42	5.20	35260.62	35200.12
Shelf (erosion–deposition) (10^6 t y^{-1})	−3.05	9.19	0.35	9.54	9.31
Shelf export (10^6 t y^{-1})	0.40	8.45	0.41	8.85	8.85

Scenarios with natural (waves and currents) and/or trawling resuspension include sediment input by rivers. Deposition and export rates for these scenarios exclude the deposited and exported sediment directly deriving from rivers. Once riverborne sediment has been deposited on the shelf it is accounted for in the resuspension, and subsequent deposition and export fluxes.

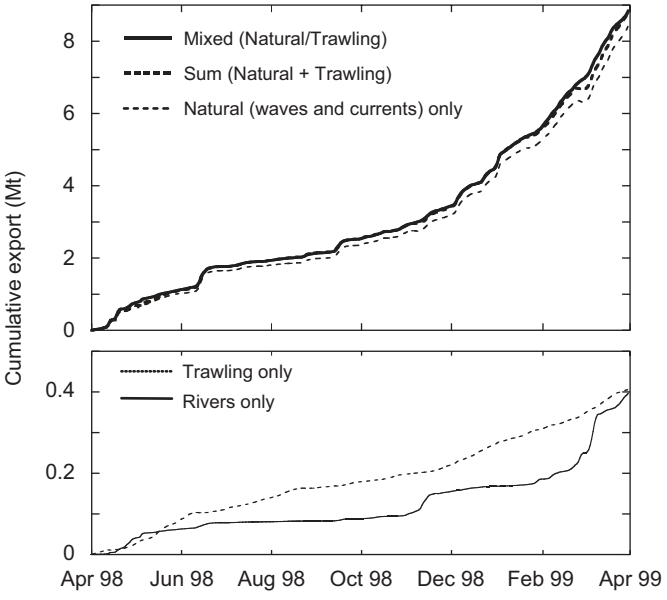

Fig. 5. Cumulative export (in 10^6 metric tonnes) for the different scenarios: rivers only (without resuspension), naturally induced (waves and currents) resuspension only, trawl-induced resuspension only and mixed (waves, currents and trawls) resuspension. The thick dashed line indicates the sum of export for scenarios with natural (waves and currents) only and trawl-induced only scenarios.

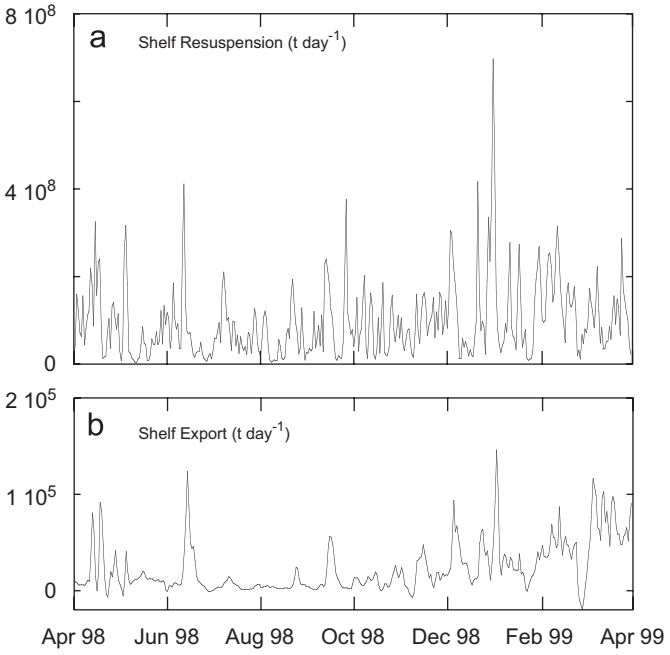

Fig. 6. Annual (from April 1, 1998 to March 31, 1999) variability of the mass of sediment resuspended daily by waves and currents on the Gulf of Lion's shelf (a) and exported from the shelf using the limits depicted in Fig. 1 (b).

duration of a few days, throughout the year. Some larger and longer resuspension events were noted in spring and fall 1998, and also during December 1998 and February 1999, due to the action of stronger coastal currents or swells. During the April 1998–April 1999 period about 35.3×10^9 t of sediment were resuspended (Table 2), preferentially on the inner shelf (water depth < 50 m) (Fig. 7), and the largest part was composed of coarse sediments that quickly settled. The annual net erosion/deposition budget amounted to 9.2×10^6 t (Table 2), which was more than twice the annual river inputs.

Off-shelf export occurred as bursts, which immediately followed the resuspension events. They were generally of short duration except for a sustained period in February and March 1999 due to dense shelf water cascading (Fig. 6b). Water flux at the shelf break (Fig. 3g) indicated that the two summer pulses on mid-June and mid-September 1998 occurred on the eastern part of the Gulf, while all the other episodes occurred in its western part. The annual export of sediment solely resuspended by waves and currents amounted to 8.5×10^6 t (Fig. 5), which represented about 0.02% of the resuspended quantity (Table 2). The exported sediment was mostly composed of clays and fine silts, but the strong cascading-driven currents induced an export of larger particles (including sands) during the winter 1999.

The map of erosion and deposition regions at the end of the annual cycle (Fig. 7) indicated a net deposit over most of the shelf, except within the coastal band shallower than 30 m, and also on the southwestern outer shelf.

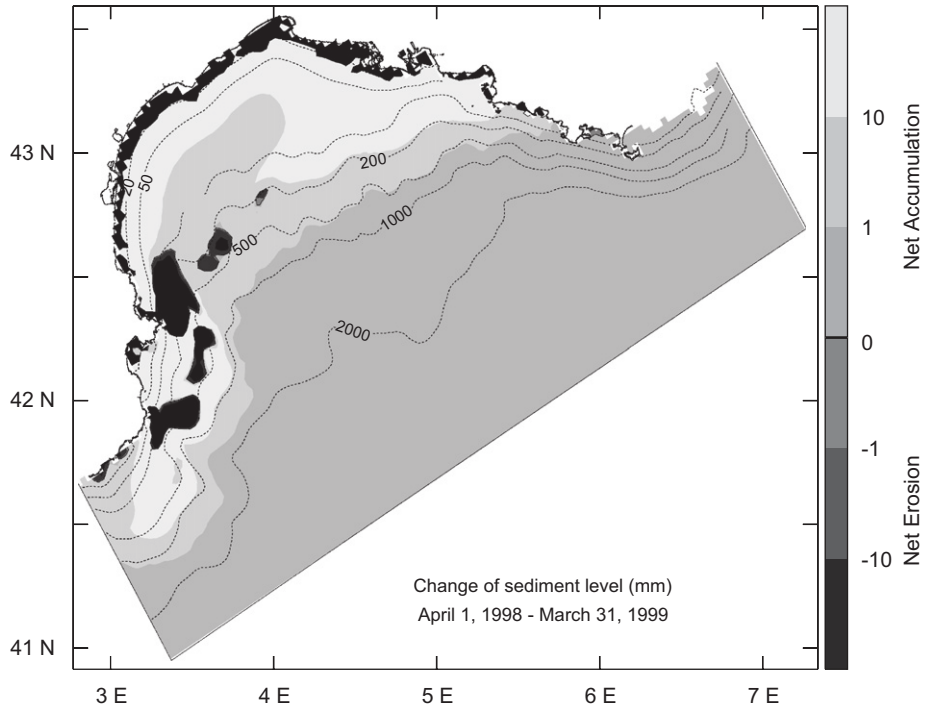

Fig. 7. Map of sediment thickness accumulated or eroded between April 1, 1998 and March 31, 1999 taking into account sediment discharges from all rivers and resuspension by waves and currents. The contours are in mm, positive values (light areas) represent deposition and negative values (dark areas) represent erosion.

Resuspension by waves and currents induced a total redistribution of the riverine sediments, but did not significantly change the initial grain size distribution of the shelf sediments (i.e., cross-shelf gradient with coarser sediment near the coast and finer sediment seaward). Regions of stronger deposition were localised along a band between depths of 30 and 70 m, extending from the Rhône River as far as Cape Creus, which constitutes a natural outlet at the southwestern end of the Gulf. This band, which mimics the mid-shelf mud belt, was primarily composed of fine particles. Distinct patches of deep erosion of sediment by waves and currents were confined to the western gulf and extended to the 500-m isobath. This erosion occurred mainly during the winter cascading period and is related to the convergence and acceleration of dense bottom flow toward the southern end of the shelf and down the head of the canyons.

The dispersal of suspended sediment on the slope was variable according to the period of the year. From May to November, while the water column was stratified, the export of shelf suspended sediment was primarily restricted to the surface slope waters (Fig. 8a). The seaward dispersal in the upper layer (0–500 m) was limited by the core of the permanent cyclonic Northern Current that swept the material escaping from the shelf along the slope. From December to April, while the water column was weakly stratified or even unstable during the dense water cascading period, shelf suspended sediment rapidly spread into intermediate (500–1000 m) or deep (>1000 m) slope waters (Fig. 8b).

4.3.2. Resuspension and off-shelf sediment export induced by trawls

In contrast to natural resuspension which occurs as irregular and short episodes, bottom trawling activity is periodic and rather constant over the whole year (Fig. 3d). Resuspension by trawls is dependant on the trawl number and positions. During the April 1998–April 1999 period, bottom trawlers worked 250 days and the fishing fleet had a daily mean strength of 63 boats. The total surface scraped by trawlers during this annual period amounted to 11,000 km^2, which is comparable to the surface of the Gulf of Lion shelf (ca. 12,000 km^2). Some regions were trawled several times a year, whereas others were untouched. For strong winds ($>10\,m\,s^{-1}$), trawlers were mostly confined to the coastal area, where coarse sediment is more abundant (Fig. 2a). Days of strong winds were present 13% of the year, most of the time in autumn and winter. During low wind periods ($\leqslant 10\,m\,s^{-1}$), trawlers preferentially worked on the outer shelf and eroded finer sediment (Fig. 2b). About 2.2×10^4 t of sediment was resuspended daily by bottom trawls (Fig. 9a), with a maximum between September and December 1998 when trawlers were more numerous (>80, Fig. 3d). The sawtooth pattern is related to the trawling activity that stops during weekends and holidays. The annual mass of sediment resuspended by trawling amounted to 5.6×10^6 t (Table 2), most of it originating from depths between 80 and 130 m (Fig. 10). Considering the fraction that settled shortly after resuspension, the annual net erosion/deposition budget on the shelf amounted to 0.4×10^6 t (Table 2), which was one order of

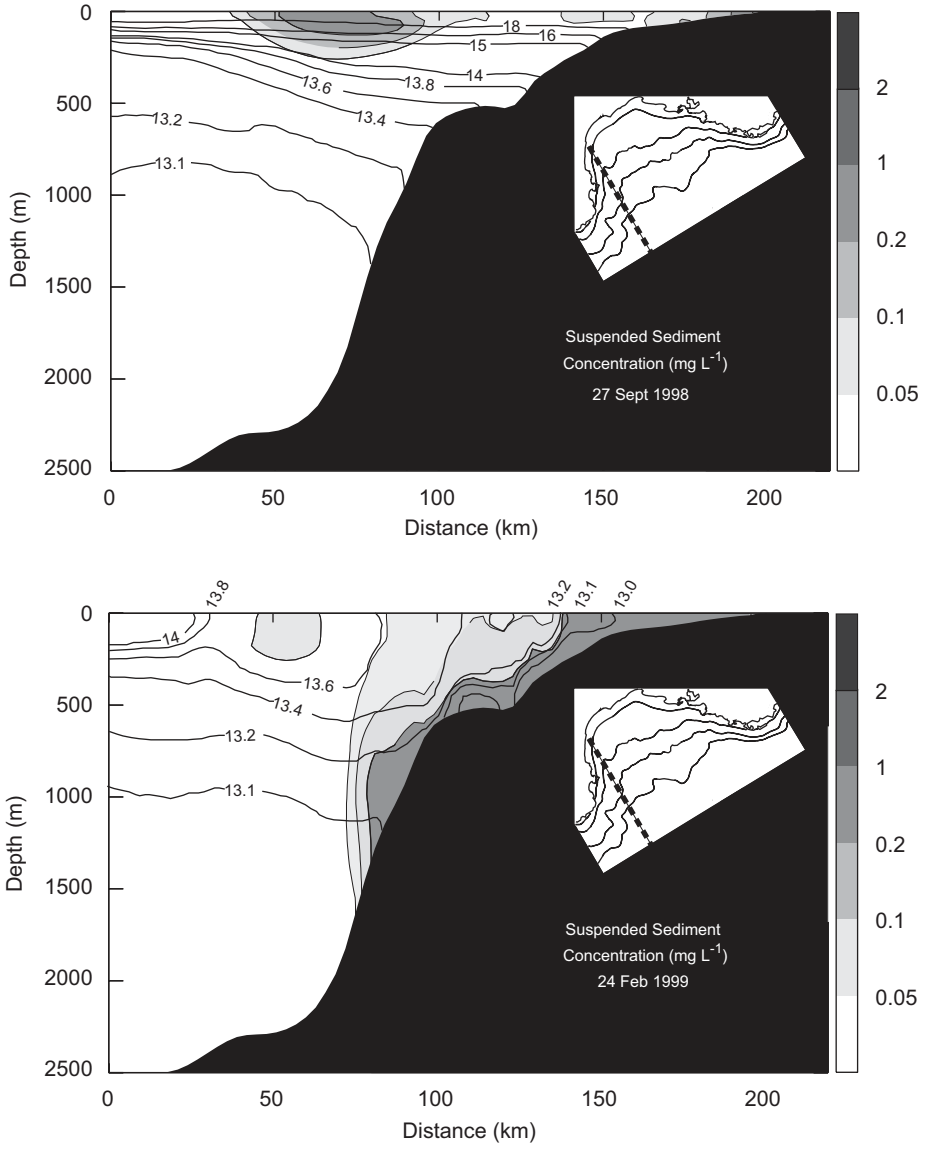

Fig. 8. Cross-margin sections on the western part of the Gulf of Lion (see Fig. 1 for section position) showing the distribution of suspended sediment concentration, resuspended by waves and currents, along with water temperature in (a) strongly stratified conditions of the upper water column (September 27, 1998) and (b) weakly stratified conditions (February 24, 1999). The contour unit is mg L^{-1}. The inserted map indicates the location of the cross-slope transect.

magnitude less than that induced by wave- and current-induced resuspension.

The export of resuspended sediment from the shelf showed a seasonal variability, with minimum fluxes during summertime (while the trawling-induced resuspension on shelf was maximum), and a significant increase arising from transport pulses during the winter and spring periods (Fig. 9b). The fine-grained sediment resuspended by trawlers on the outer shelf was exported primarily in the western half of the Gulf (Fig. 10). The off-shelf export added up to 0.4×10^6 t annually, which accounted for ~7% of the quantity of sediment resuspended by trawling on the shelf (Table 2; Fig. 5).

Transects showed that the cross-slope dispersal of the fine-grained sediment resuspended by trawlers went deeper than for the sediment resuspended by waves and currents, due probably to the proximity of regions of intense trawling activity with the shelf edge. Some sediment settled to depths of 1500–2000 m during summer stratified condition (Fig. 11a). Cascading of dense water during winter caused a rapid advection of turbid shelf water down to 1000 m deep, and settling favoured the spreading of suspended sediment as far as 2000 m deep (Fig. 11b). Above the bottom layer, suspended particles present in intermediate and deep waters were advected toward the southwest by the general along-slope circulation.

4.3.3. *Resuspension and off-shelf sediment export induced by both waves/currents and trawls*

A simulation including both natural (waves and currents) and anthropogenic (trawling) processes was intended to check if our assumption about the independence on sediment transport was justified. By comparison with the

sum of both processes, the annual resuspension and deposition on the shelf due to the combined effect of waves/currents and trawls decreased by ~0.17%, and the off-shelf export did not change (Table 2).

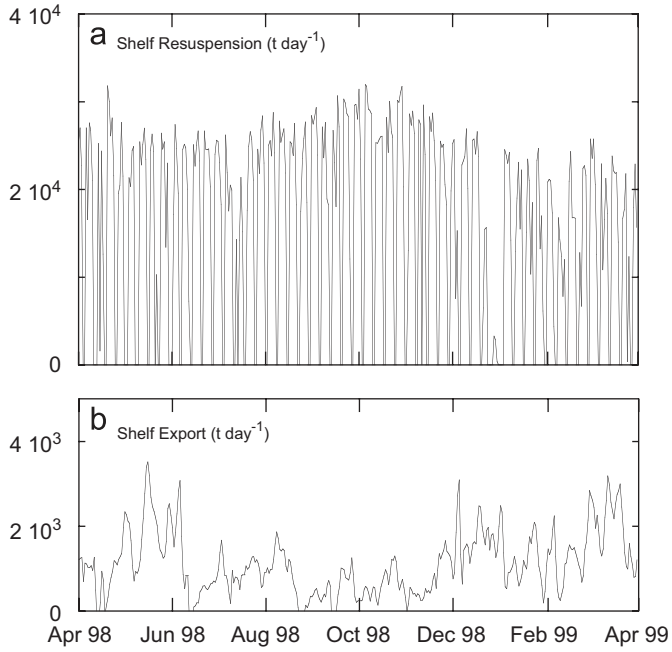

Fig. 9. Annual (from April 1, 1998 to March 31, 1999) variability of the mass of sediment resuspended daily by bottom trawlers on the Gulf of Lion's shelf (a) and exported from the shelf using the limits depicted in Fig. 1 (b). Trawling activity occurs every day except during weekends and holidays.

The resulting impact of both resuspension processes in the annual change in sediment level is depicted in Fig. 12. By comparison with the impact of each individual resuspension process (Figs. 7 and 10), the net erosion/deposition intensity is smoothed all over the shelf. The major areas of net erosion appeared along the coast, as well as on the western outer shelf and around the Cape Creus at the southwestern end of the Gulf. Net sediment accumulation took place over most of the middle shelf and eastern shelf, especially between depths of 20 and 50 m.

In the model, trawling-induced resuspension produces over time a slight coarsening of the sediment in the fishing grounds. The impact of bottom trawling activity on the sediment grain size has been already observed in other regions. Brown et al. (2005) showed on the southeastern Bering Sea that an area protected from bottom trawling, but subjected to natural resuspension as the entire coastal region area, had a significantly finer grain size owing to the lack of winnowing impact of trawling-induced resuspension. Thus some synergist effects between natural and trawling resuspension exist, but they do not significantly change the net erosion and export fluxes for the Gulf of Lion.

5. Discussion

5.1. Comparison of sediment resuspension by waves/currents and trawls

On average, the amount of sediment resuspended by waves and currents exceeds by three to four orders of

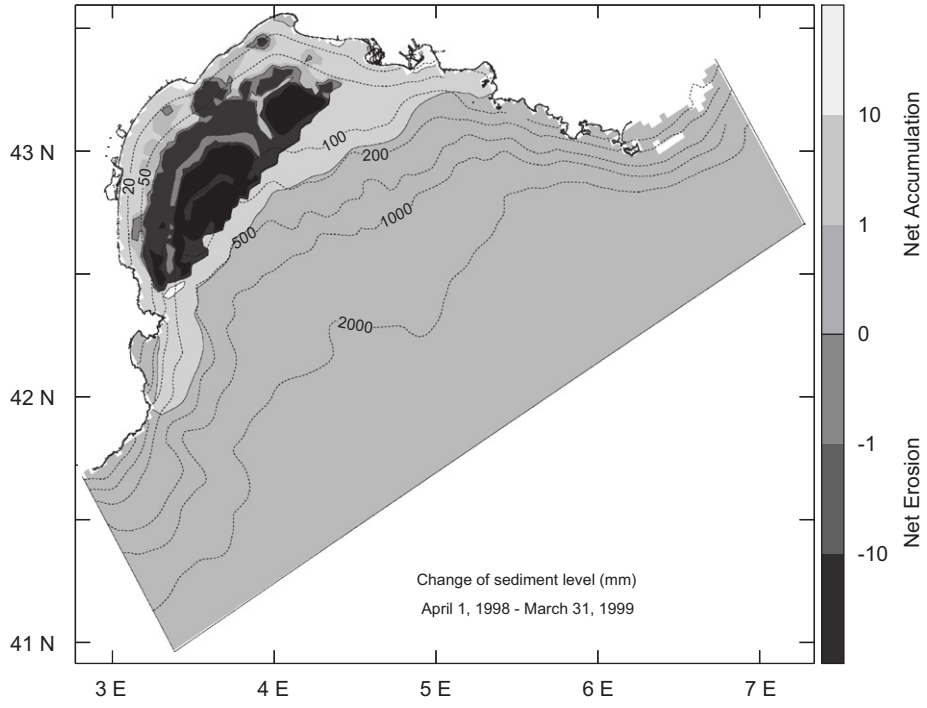

Fig. 10. Map of sediment thickness accumulated or eroded between April 1, 1998 and March 31, 1999 taking into account sediment discharges from all rivers and resuspension by bottom trawling. The contours are in mm, positive values (light areas) represent deposition and negative values (dark areas) represent erosion.

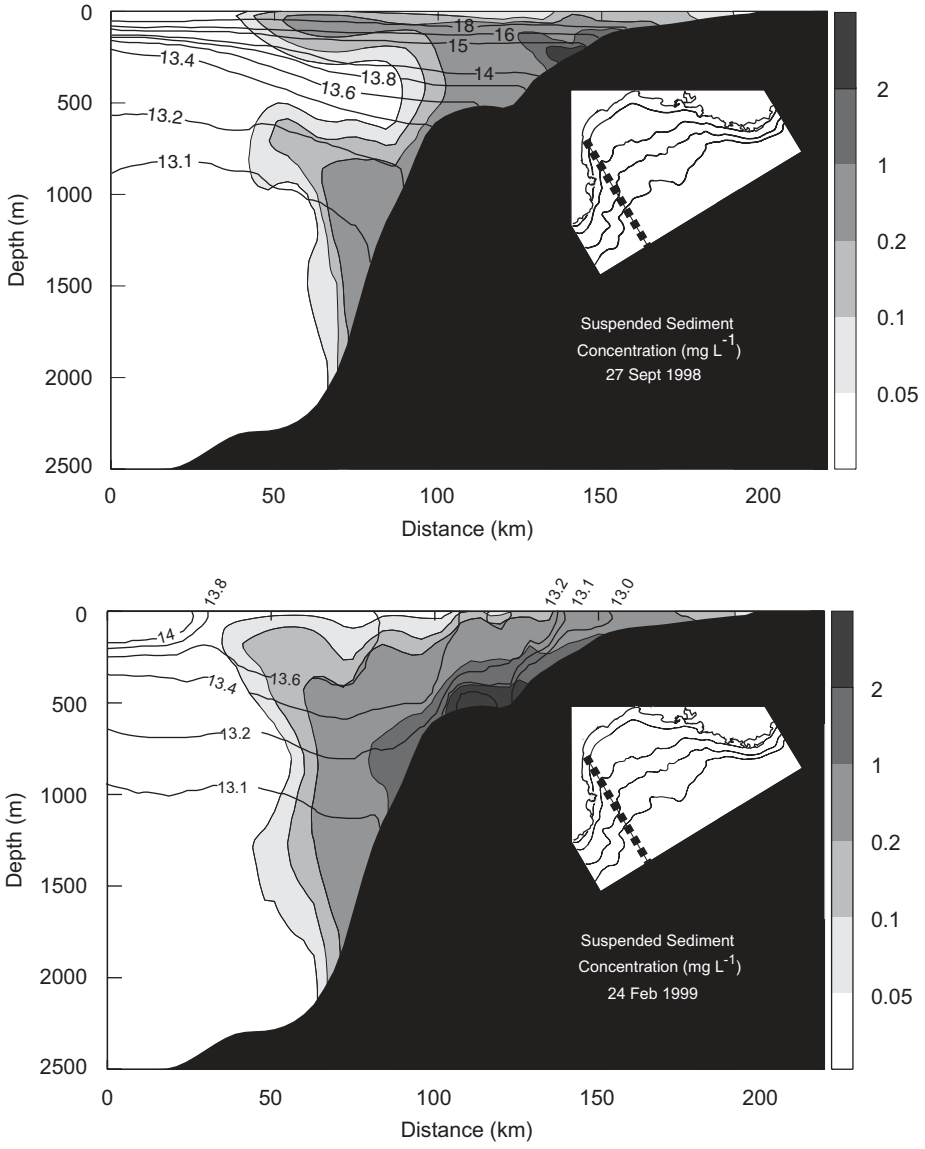

Fig. 11. Cross-margin sections on the western part of the Gulf of Lion (see Fig. 1 for section position) showing the distribution of sediment concentration, resuspended by bottom trawling, along with water temperature in (a) strongly stratified conditions of the upper water column (27 September 1998) and (b) weakly stratified conditions (24 February 1999). The contour unit is mg L^{-1}. The inserted map indicates the location of the cross-slope transect.

magnitude those induced by trawling (Table 2). By calculating the suspended mass per bottom eroded area for annual and winter/summer periods, a comparison can be made between depths eroded by waves and currents, and by trawls (Fig. 13).

Wave and current resuspension flux strongly decreases with increasing water depth, because of the decreasing impact of wave motions, and stabilises on the outer shelf where strong bottom currents still resuspend muddy sediments (Fig. 13a). Seasonal (winter and summer) fluxes in shallow water are comparable, but summer fluxes decrease more rapidly offshore due to the weaker bottom current intensity. Ulses et al. (this issue) and Dufois et al. (this issue) also demonstrate for different periods (2001 and 2003–2004, respectively) that bottom-shear stress and sediment erosion were primarily controlled by waves on the inner shelf and by energetic wind-driven currents on the outer shelf.

Resuspension fluxes induced by trawling are maximum on the outer shelf (between 80 and 130 m of depth) and culminate around 100 m depth (Fig. 13b). Seasonally, fluxes are weaker during the winter period by a factor of about 2, because poor sea conditions reduce the average number of sea trips (Fig. 3d). On a yearly basis, resuspension fluxes generated by trawls on the outer shelf are lower than the fluxes generated at the same depths by waves and currents. However, the trawling-induced fluxes significantly exceed the wave- and current-induced fluxes during summertime.

Churchill (1989) suggested, by comparing temporally averaged sediment loads (per unit bottom area) calculated using a simple model, that waves and currents on the

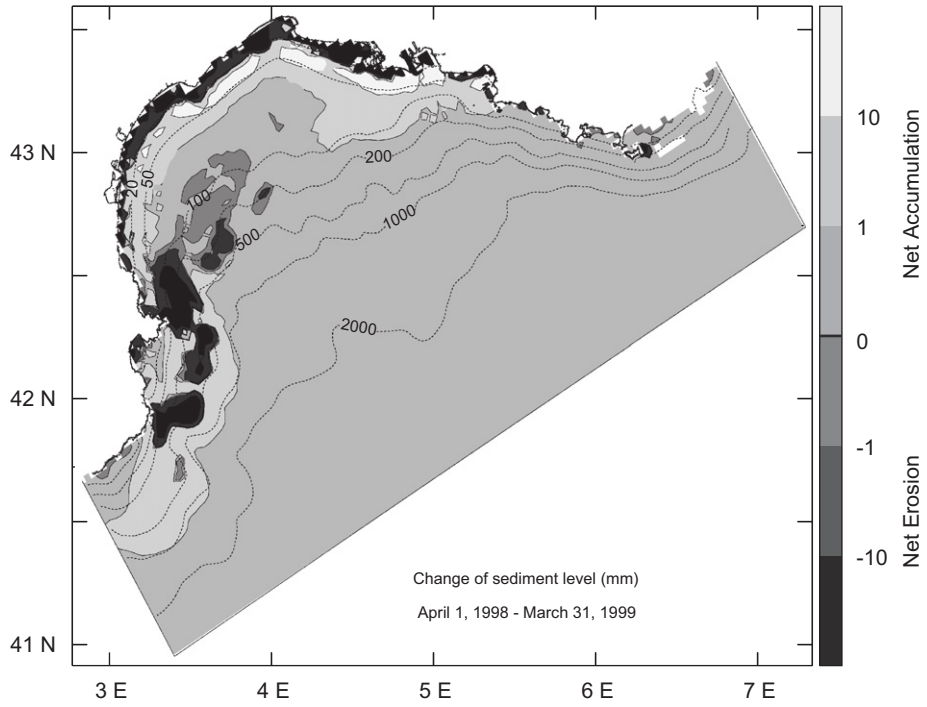

Fig. 12. Map of sediment thickness accumulated or eroded between April 1, 1998 and March 31, 1999 taking into account sediment discharges from all rivers and both resuspension by waves and currents, and bottom trawling. The contours are in mm, positive values (light areas) represent deposition and negative values (dark areas) represent erosion.

mid-Atlantic Bight were responsible for the resuspension on the inner shelf shallow water, whereas trawling was the principal cause of resuspension on the outer shelf. Our computations of temporally integrated resuspension fluxes show qualitatively similar results. In particular, both approaches emphasise the larger impact of bottom trawling on sediment remobilisation in deep regions of the continental shelf. However, the magnitude of the trawling contribution in Churchill's work seems to be significantly greater than the present study. This can relate to the different methods of calculation, but also from different seafloor characteristics, as the Gulf of Lion shelf is mainly made up of fine sediments (clays and silts), whereas sands primarily dominate the seafloor of the Mid-Atlantic Bight.

5.2. Impact on sedimentary budget

The main export pathways differ for naturally or trawling-induced resuspended sediments because of the different resuspension regions. Waves and currents resuspend sediment mostly on the inner shelf, where it is composed of coarser grains that quickly settle. The fine fraction is then primarily transported along shore toward the southwestern end of the Gulf where it escapes the shelf. Conversely, fine sediment resuspended by trawls is mostly exported to the central slope, owing to the fact that trawled regions are mainly located on the outer shelf, close to the shelf break.

Whereas resuspension induced by waves and currents usually dwarfs that induced by trawling, the net erosion (i.e., resuspension-deposition) and the export are more comparable (Table 2). Indeed, sediments resuspended by trawls contribute to about 5% of the annual total export of riverborne and resuspended sediment of the Gulf of Lion shelf (Table 2; Fig. 5). Nevertheless, this export shows an important seasonal and interannual variability due to the storm frequency and intensity, resulting in a variable contribution of trawling to the export.

During summertime the effect of waves and currents is minimal while the activity of trawling is maximum. Quantitatively, these conditions induce an increased contribution from trawling, which reaches 7% of the total export for the period April 1998–September 1998. During wintertime the contribution of trawling reaches a minimum of around 4%.

Ulses et al. (submitted for publication) estimated—using a similar modelling approach—sediment resuspension and export by waves and currents for the Gulf of Lion for the November 2003–May 2004 period. This latter period was characterised by large river discharges and E–SE storm activity, with the occurrence of one major flood and two extreme storms, but mild dense water formation and export. It was quite different from the low river discharges, low E–SE storm activity, but massive dense shelf water cascading 1998–1999 winter period addressed in the present study. The amount of sediment exported during comparable time period reveals that the export during the

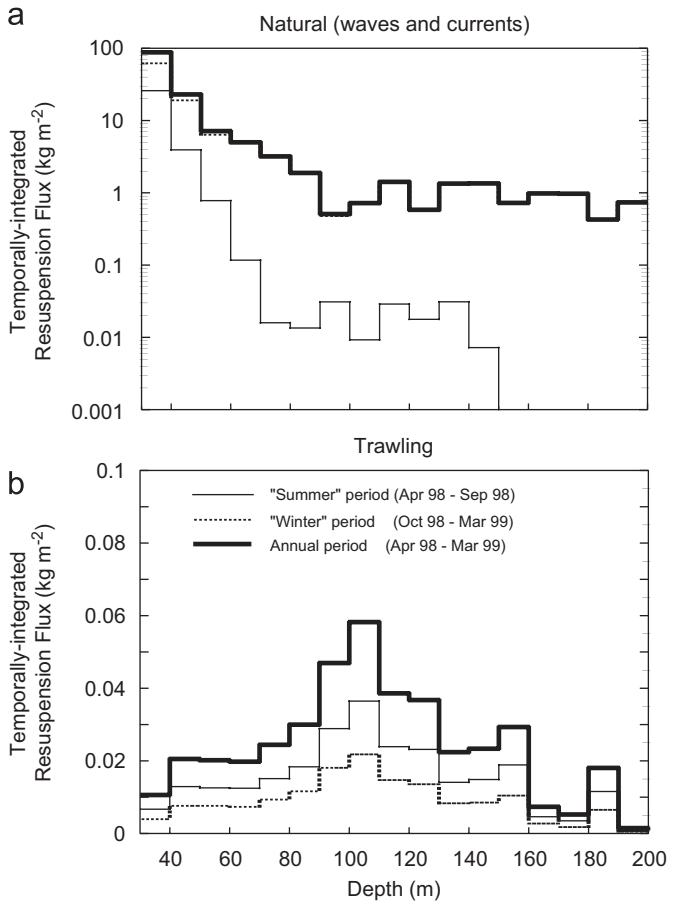

Fig. 13. Annual and seasonal variation with depth of the temporally integrated resuspension fluxes on the Gulf of Lion's shelf linked (a) to natural (wave and current) activity and (b) to bottom trawling activity. The first 30 m depths are not represented because of the strong erosion by waves and currents very near the coast which dwarfed the other values.

November 2003 and March 2004 period (8.6×10^6 t) was larger than during the 1998–1999 period (5.7×10^6 t between November 1998–March 1999). The 1998–1999 and 2003–2004 periods were very energetic and are believed to represent the upper range of the export. On the other side, Durrieu de Madron et al. (2000) estimated, using a box model budgeting approach based on direct measurements performed during two seasonal surveys, an annual export of suspended particulate matter of about 1.9×10^6 t. This crude estimate is believed to represent the lower range of the export, as surveys were performed in 1995–1996 during relatively calm conditions. Assuming that the export of sediment associated to the trawling activity is relatively constant from 1 year to the other (i.e., of the order of 0.4×10^6 t), we estimate that this activity could contribute between a few and 20% of the annual shelf-to-slope exchange of suspended sediment at the scale of the Gulf.

6. Conclusions

Resuspension and transport of sediment in the Gulf of Lion, due to waves and currents and to trawling, have been modelled for an annual period (April 1998–April 1999). The major conclusions that can be drawn with these results are:

- Natural resuspension by waves and currents occurred during short episodes mostly during fall and winter. It was concentrated on the inner shelf due to wave action, but also on the southwestern outer shelf due to the strong bottom currents occurring during wintertime. Trawling-induced resuspension occurred regularly throughout the year. It was concentrated on the outer shelf, with a maximum intensity around 90 m depth. Trawling-induced resuspension fluxes are on average several orders of magnitude lower than the wave- and current-induced resuspension fluxes. Nevertheless, they are maximum and locally predominant during summertime when the wave and currents activity is lowest.
- The total annual off-shelf export of sediment by waves and currents was one order of magnitude larger than the export linked to trawling. Export concerned the finest fraction of the sediment (clays and fine silts) and took place primarily in the southwestern end of the Gulf for the sediment resuspended by waves and currents and the outer shelf for the sediment resuspended by trawling. During energetic years (i.e., with large flood, strong marine storm or dense water formation), trawling activity contributed little (a few percent) to the total shelf export of fine sediment. However, trawling was thought to contribute significantly (up to 20% of the export) during calm years.
- No significant interferences between both resuspension processes were estimated in terms of resuspension/deposition and export fluxes.

Because of the site-specific characteristics of natural resuspension and transport mechanisms, morphological and sedimentological settings, intensity and distribution of the trawling effort, all the conclusions obtained for the Gulf of Lion may not necessarily apply to other continental shelves. Nevertheless, the depth limitation of resuspension by waves and the increasing impact of trawling in deeper portions of the shelf-where natural resuspension processes become tenuous—are likely to be features common to most coastal regions with significant bottom trawling activity.

Acknowledgements

The authors acknowledge the support from the European Commission (INTERPOL Project under contract EVK3-2000-00023 and EUROSTRATAFORM Project under contract EVK3-CT-2002-00079). We thank Patricia Wiberg and two anonymous reviewers for their constructive and valuable comments.

Appendix A

Suspended sediment transport equation

The advection-diffusion equation is based on the mass conservation of the suspended sediment

$$\frac{\partial C^i}{\partial t} + u\frac{\partial C^i}{\partial x} + v\frac{\partial C^i}{\partial y} + (w - W_s^i)\frac{\partial C^i}{\partial z} = K_z\frac{\partial^2 C^i}{\partial z^2}, \quad (A.1)$$

where C^i is the suspended sediment concentration (SSC) for the ith class of particles, W_s^i is the settling velocity, u, v and w are the horizontal and vertical velocities, respectively, and K_z is the vertical diffusion coefficient.

The vertical turbulence was estimated using a turbulent closure scheme where the vertical diffusion coefficient K_z is derived from the local Richardson number ($Ri = -((g/\rho)/(\partial\rho/\partial z))/(\partial u/\partial z)^2$) (Munk and Anderson, 1948):

$$K_z = 1.67 \times 10^{-3}\left(1 + \frac{10}{3}Ri\right)^{-3/2}, \quad (A.2)$$

where ρ is the water density and g is the gravitational acceleration equal to $9.81\,\mathrm{m^2\,s^{-1}}$.

Settling velocity W_s^i (in $\mathrm{m\,s^{-1}}$) for the particles with a diameter lower than 100 μm was estimated as the mean Stokes velocity of the individual size bins D_j (in m):

$$W_s^i = \frac{(s_i - 1)gD_i^2}{18v}, \quad (A.3)$$

where s_i is the relative grain density and v is the kinematic water viscosity equal to $1.14 \times 10^{-6}\,\mathrm{m^2\,s^{-1}}$.

Settling velocity for sand grain coarser than 100 μm is computed using Zanke (1977) formula:

$$W_s^i = \frac{10v}{D_i}\left\{\left[1 + \frac{0.01(s_i - 1)gD_i^3}{v^2}\right]^{0.5} - 1\right\}. \quad (A.4)$$

Settling velocity of aggregates is computed using the relationship from Agrawal and Pottsmith (2000):

$$W_s^i = 0.45 \times 10^{-3}\left(\frac{D_i}{2}\right)^{1.17}, \quad (A.5)$$

where W_s^i and D_i are expressed in $\mathrm{cm\,s^{-1}}$ and μm, respectively.

Density of primary particles is taken as the mineral grain density ($2640\,\mathrm{kg\,m^{-3}}$) and density of aggregates is calculated according to Hill et al. (1998):

$$\rho_f^i = \rho + \frac{18\mu W_s}{gD_f^2}\left(1 + \frac{3C}{16}Re\right), \quad (A.6)$$

where ρ_f^i is the aggregate density, μ is the dynamic water viscosity ($1.14 \times 10^{-3}\,\mathrm{kg\,m^{-1}\,s^{-2}}$), W_s is the aggregate settling velocity, D_f is the aggregate diameter, C is the Carrier coefficient (0.43) and $Re = \rho W_s^i D_f^i/\mu$ is the class i Reynolds number.

Appendix B

Erosion flux for trawling

The fluxes of sediment resuspended by bottom trawls were estimated experimentally and presented in Durrieu de Madron et al. (2005). By comparing resuspension by two different configurations of groundrope gear (chain or "rock hopper" fixed rubber discs), working at a speed of 3 knots over the ground, with an average net aperture and door width of 16 m, they showed that resuspension by trawling depends on the trawl's goundrope, but above all on the sediment texture (clay content). A linear relationship is inferred between the total resuspension flux, E_T in $\mathrm{kg\,m^{-2}\,s^{-1}}$, and the clay fraction, F_C in %:

$$E_T = 0.01F_C + 0.47 \quad (r^2 = 0.74).$$

Total flux is then fractionated for the different sediment grain sizes, according to the fraction p_i of class i:

$$F^i = p_i E_T.$$

Erosion fluxes for waves and currents

Partheniades' law for cohesive sediments

We calculate the erosion flux F for each particle class i according to the relation:

$$F^i = p_i E_0^i\left(\frac{\tau_{\max,s}}{\tau_{cr_i}} - 1\right) \quad \text{if } \tau_{\max,s} \geqslant \tau_{cr_i}, \quad (B.1)$$

where τ_{cr_i} is the critical shear stress for the class i and p_i is the fraction of class i. The erosion coefficient E_0 depends on the physico-chemical sediment characteristics and ranged between 10^{-5} and $2 \times 10^{-3}\,\mathrm{kg\,m^2\,s^{-1}}$ (Mulder and Udink, 1991; Amos et al., 1992, 1997; Widdows et al., 1998). In this study, the coefficient E_0 was set to $1 \times 10^{-5}\,\mathrm{kg\,m^2\,s^{-1}}$.

Reference concentration method for non-cohesive sediments

We calculate the erosion flux F for each particle class i according to the relation:

$$F^i = p_i W_s^i C(z_1)\rho_s^i, \quad (B.2)$$

where $C(z_1)$ is an a dimensional concentration at the height z_1 corresponding to the first layer of the grid of above the seabed. Under combined wave and currents conditions, sediment is resuspended within the wave boundary layer and diffused in the water column by turbulence associated with the current (Soulsby et al., 1993). In the model, height of the first layer (z_1) is variable and can be above the wave boundary layer of thickness z_w. The concentration $C(z_1)$ is thus calculated according to the reference concentration C_a, at height $z_a = 2D_{50}$, or the concentration at the boundary layer level $C(z_w)$.

$$C(z_1) = \begin{cases} C_a\left(\frac{z_1}{z_a}\right)^{-b_{\max}} & \text{for } z_a \leqslant z_1 \leqslant z_w, \\ C(z_w)\left(\frac{z_1}{z_w}\right)^{-b_m} & \text{for } z_w < z_1. \end{cases}$$

with

$$b_{\max} = \frac{W_s}{\kappa u_{*\max}} \quad \text{and} \quad b_m = \frac{W_s}{\kappa u_{*m}},$$

$$z_w = \frac{u_{*\max} T}{2\pi} = \text{wave boundary thickness.}$$

W_s is the sediment settling velocity, κ is the von Karman constant ($=0.40$), $u_{*\max} = (\tau_{\max}/\rho)^{1/2}$, $u_{*m} = (\tau_m/\rho)^{1/2}$, $\tau_{\max}$ is the maximum bed shear-stress in wave cycle, τ_m is the mean bed shear-stress in wave cycle, and T the wave period.

The determination of the reference concentration is based on the Zyserman and Fredsøe (1994) method, and is calculated for a grain-related roughness height of $2.5 \times D_{50}/30$:

$$C_a = \frac{0.331(\theta_{\max,s} - 0.045)^{1.75}}{1 + 0.720(\theta_{\max,s} - 0.045)^{1.75}}, \tag{B.3}$$

where $\theta_{\max,s} = \tau_{\max,s}/g(\rho_s - \rho)D_{50}$ is the skin-friction Shields parameter. This method is designed for flat-bed condition, so that $\tau_{\max}$ and τ_m are calculated using a grain related roughness height ($2.5 \times D_{50}/30$). For a rippled bed, total-stress values should be used.

Critical shear stress

The critical shear stress is the shear stress at which sediment is likely to be mobilised. It depends on the grain itself and on bottom characteristics. This value is difficult to establish because it can vary from a factor 10–20 according to the type of resuspension considered.

For coarse non-cohesive sediments, critical shear stress of each class i is given in form of a critical Shields parameter value θ^i_{cr} which depends on a dimensional grain size and results from experiments. Soulsby and Whithouse (1997) determined an algebraic equation nearest to the Shields curve:

$$\theta^i_{cr} = \frac{0.30}{1 + 1.2D^i_*} + 0.055[1 - \mathrm{e}^{-0.020D^i_*}], \tag{B.4}$$

where

$$D^i_* = \left[\frac{g(s^i - 1)}{\nu^2}\right]^{1/3} D^i_{50}.$$

Critical shear stress τ^i_{cr} is thus calculated with the equation

$$\theta^i_{cr} = \frac{\tau^i_{cr}}{g(\rho^i_s - \rho)D^i_{50}}. \tag{B.5}$$

Roughness and bedforms

For non-cohesive sediments, total bottom roughness is computed using the relationship

$$z_0 = \frac{k}{30}, \tag{B.6}$$

where k is the total roughness height, and is the sum of three components: grain-related component (k_g), bedload component (k_t), and form-drag component (k_f) (Grant and Madsen, 1982).

$$k = k_g + k_t + k_f. \tag{B.7}$$

Grain roughness height is calculated using:

$$k_g = 2.5 \times D_{50}. \tag{B.8}$$

Bedload roughness is calculated using:

$$k_t = 522 \times D_{50}(\theta_{cws} - \theta_{cr})^{0.75}. \tag{B.9}$$

where $\theta_{cws} = \rho u^2_{*cws}/(\rho_s - \rho)gD_{50}$ is the Shields parameter related to the skin roughness, θ_{cr} is the critical Shields parameter which define grains remobilisation, and U_{*cws} is combined wave and currents shear velocities. Ripple height and wavelength are then calculated according to Li and Amos (1998) (see below) to obtain the form-drag roughness height

$$k_f = \frac{a_r \eta^2}{\lambda}, \tag{B.10}$$

where a_r is a coefficient which varies according to authors. We choose 27.7, the most common value, fixed by Grant and Madsen (1982).

The ripple height and wavelength depend on the sediment characteristic and hydrodynamical conditions. Skin shear velocities (u^*_{cws}) and skin-friction combined wave and current Shields parameter (θ_{cws}) are first calculated using the grain roughness height k_g. The bedload roughness k_t can thus be calculated, and is used to obtain bedload shear velocities (u^*_{wt}, u^*_{ct}, u^*_{cwt}). To calculate ripples dimensions, the combined-flow ripple predictor proposed by Li and Amos (1998), based on their filed observations of ripples on Scotian Shelf, is used. Ripple dimensions are calculated according to five limiting conditions that depend on four friction velocities: ripple-enhanced shear velocity (u_{*cwe}; Nielsen, 1986), critical shear velocity for bedload transport (u_{*cr}), critical shear velocity for ripple break-off (u_{*bf}; Grant and Madsen, 1982) and critical shear velocity for upper-plane bed sheet-flow (u_{*up}). This last variable is given from a data compilation from preceding studies, carried out by Li and Amos (1998). The friction velocities are calculated as: $U_{*cwe} = u_{*cws}/(1 - \pi\eta_p/\lambda_p)$ where η_p and λ_p are, respectively, height and wavelength of pre-existing ripples. $u_{*cr} = \sqrt{\tau_{cr}/\rho}$, τ_{cr} being the critical shear stress for erosion as explain hereafter. $u_{*bf} = 1.34S^{0.3}_* u_{*cr}$ where $S_* = (D_{50}/4\nu)[(\rho_s - \rho)gD_{50}/\rho]$ is without dimension and ν is the cinematic seawater viscosity (equal to 1.14×10^{-6} for a 15 °C seawater). $u_{*up} = \sqrt{\tau_{up}/\rho}$ where $\tau_{up} = \theta_{up}(\rho_s - \rho)gD_{50}$ and $\theta_{up} = 0.172D^{-0.376}_{50}$, D_{50} is expressed in mm.

The five limiting conditions presented below permit us to calculate ripples height η_{rip} and wavelength λ_{rip}:

(1) If $u_{*cwe} < u_{*cr}$, there is no sediment transport and ripples have the same dimension as precedent time step.

(2) If $u_{*cwe} > u_{*cr}$ and $u_{*cws} < u_{*cr}$, the transport is local, weak, and close to ripples crest.
- $\eta_{rip}/D_{50} = 19.59\ (u_{*cws}/u_{*cr}) + 20.92$,
- $\eta_{rip}/\lambda_{rip} = 0.12$.

(3) If $u_{*cws} > u_{*cr}$ and $u_{*cwt} < u_{*bf}$, overall bedload transport will occur.
- Case no. 1: $u_{*cw}/u_{*cs} \geqslant 1.25$, wave-dominant ripples
  - $\eta_{rip}/D_{50} = 27.14\ (u_{*cwt}/u_{*cr}) + 16.36$,
  - $\eta_{rip}/\lambda_{rip} = 0.12$.
- Case no. 2: $u_{*cw}/u_{*cs} < 1.25$, current-dominant ripples or interaction between wave and currents
  - $\eta_{rip}/D_{50} = 22.15\ (u_{*cwt}/u_{*cr}) + 6.38$,
  - $\eta_{rip}/\lambda_{rip} = 0.12$.

(4) If $u_{*bf} \leqslant u_{*cwt} < u_{*up}$, break-off ripples will form
- $\lambda_{rip} = 535\, D_{50}$,
- $\eta_{rip}/\lambda_{rip} = 0.15\ (u_{*up} - u_{*cwt})/(u_{*up} - u_{*bf})$.

(5) If $u_{*cwt} \geqslant u_{*up}$, ripples are washed out and upper-plane bed will be predicted.
- $\eta_{rip} = 0$,
- $\lambda_{rip} = 0$.

From these ripples height and wavelength values, the drag roughness, and then the total bottom roughness can be calculated, giving access to the calculation of the bottom-shear stress which will determine the reference concentration.

For cohesive sediment, biological activity can have a considerable effect on bottom roughness. Microbial exudates can increase the critical shear stress, and the presence of burrows in the sediment, due to bioturbation, can strengthen the seabed (Meadows et al., 1990; Black, 1997). Because data concerning biological roughness are non-existent in the Gulf of Lion, ripple height and wavelength for cohesive sediment are here set equal to those measured on a silty site in the northern California shelf (0.6 and 10 cm, respectively; Wheatcroft, 1994). The steepness of biogenic roughness elements is assumed to decay under high shear stresses as (Harris and Wiberg, 2001):

$$\frac{\eta_{bio}}{\lambda_{bio}} = \exp(-1.67 \ln \theta_w - 4.11), \tag{B.11}$$

where $\theta_w = \tau_{*w}/g(\rho_{s-\rho})D_{50}$.

For mixed sediment, an average between silty-bed and sandy-bed roughness scales is used, weighted by sand fraction of the bed (Harris and Wiberg, 2001):

$$\eta = \eta_{rip} fr_s + \eta_{bio}(1 - fr_s),$$
$$\lambda = \lambda_{rip} fr_s + \lambda_{bio}(1 - fr_s), \tag{B.12}$$

where fr_s is the sandy fraction. In the same way, total roughness is calculated by weighted average of the cohesive and non-cohesive contributions. A minimum value of $z_0 = 0.005$ cm is specified so that roughness estimates do not become too small given the small-scale bed variations generally present on the sea floor.

Bed armoring

We used the method of Harris and Wiberg (2001), which considers several layers below an active layer available for erosion. Underlying layers are only available when the active layer gets thinner by erosion or when shear stress increases. At the initial time, all layers (under-layers and active layer) have the same particle size distribution. The thickness and particle size distribution of each layer are updated at each time step according to deposition and erosion. The eroded volume of each particle class per unit area of seabed during a time step is limited by the quantity of sediment available in the active layer.

The active layer of sandy bottom (δ^{rip}) is calculated according to the migration rate of the bottom (Q_b) and the size of the ripples η_{rip} and λ_{rip} during a half wave period:

$$\delta^{rip} = \frac{Q_b T}{2 C_b \lambda_{rip}} + 6 D_{50}, \tag{B.13}$$

where

$$Q_b = \sum_i \left[fr_i \frac{25.3}{(\rho_s^i - \rho) g} (\tau_{cws} - \tau_{cr}^i)^{1.5} \right],$$

$$\tau_{cws} = \rho u_{*cws}^2,$$

where fr_i is the fraction of class i present in the sediment, C_b is the concentration of the sediment (1-porosity), and $6D_{50}$ represents irregularities due to grains in order to prevent the active layer to disappear when no transport occurs.

For silty sediments, the active layer depth is supposed to be proportional to the shear stress at the bottom compared to the critical shear stresses $\tau_{cr(50)}$ of the sediment:

$$\delta^{silt} = 0.006(\tau_{cws} - \tau_{cr(50)}) + 6 D_{50}. \tag{B.14}$$

For mixed sediment (mixture of silt and sand), the mixed layer δ_{mix} is calculated as a weighted mean of active layer depths for sandy and silty sediments:

$$\delta_{mix} = \delta^{rip} fr_s + \delta^{silt}(1 - fr_s). \tag{B.15}$$

where fr_s is the sand fraction of the bed. The volume of sediment available for erosion in a size class i per unit area of the bed is $fr_i C_b \delta_{mix}$. This volume is used to limit the erosion, taking into account initial sediment characteristics (critical shear stress for erosion, grain density and particle size distribution). Hence, when erosion exceeded the available sediment volume for each class i at a given site, bed armoring is applied by reducing the flux of this class.

References

Agrawal, Y.C., Pottsmith, H.C., 2000. Instruments for particle size and settling velocity observations in sediment transport. Marine Geology 168, 89–114.

Amos, C.L., Daborn, G.R., Christian, H.A., 1992. In situ erosion measurements on fine-grained sediments from the Bay of Fundy. Marine Geology 108, 175–196.

Amos, C.L., Feeney, T., Sutherland, T.F., Luternauer, J.L., 1997. The stability of fine grained sediments from the Fraser River delta. Estuarine, Coastal and Shelf Science 45, 507–524.

Arakawa, A., Suarez, M.J., 1983. Vertical differencing of the primitive equations in sigma coordinates. Monthly Weather Review 111, 34–45.

Auclair, F., Marsaleix, P., Estournel, C., 2000. Sigma coordinate pressure gradient errors: evaluation and reduction by an inverse method. Journal of Atmospheric and Oceanic Technologies 17, 1347–1367.

Béthoux, J.P., Durrieu de Madron, X., Nyffeler, F., Tailliez, D., 2002. Deep water in the western Mediterranean: peculiar 1999 and 2000 characteristics, shelf formation hypothesis, variability since 1970 and geochemical inferences. Journal of Marine Systems 33/34, 117–131.

Black, K.S., 1997. Microbiogical factors contributing to erosion resistance in natural cohesive sediments. In: Burst, N., Parker, R., Watts, J. (Eds.), Cohesive Sediments. Wiley, Chichester, pp. 231–244.

Blumberg, A.F., Mellor, G., 1987. A description of a three dimensional coastal circulation model. In: Heaps, N. (Ed.), Three Dimensional Coastal Ocean Model. 208pp.

Bougeault, P., Lacarrere, P., 1989. Parameterisation of orography-induced turbulence in a meso-beta scale model. Monthly Weather Review 117, 1872–1890.

Bourrin, F., Durrieu de Madron, X., 2006. Contribution to the study of coastal rivers and associated prodeltas to sediment supply in Gulf of Lions (N–W Mediterranean Sea). Vie et Milieu-Life and Environment 56, 307–314.

Brown, E.J., Finney, B., Dommisse, M., Hills, S., 2005. Effects of commercial otter trawling on the physical environment of the southeastern Bering Sea. Continental Shelf Research 25, 1281–1301.

Canals, M., Puig, P., Durrieu de Madron, X., Heussner, S., Palanques, A., Fabrè, J., 2006. Flushing submarine canyons. Nature 444, 354–357.

Churchill, J.H., 1989. The effect of commercial trawling on sediment resuspension and transport over the Middle Atlantic Bight continental shelf. Continental Shelf Research 9, 841–865.

DeAlteris, J., Skrobe, L., Lipsky, C., 1999. The significance of seabed disturbance by mobile fishing gear relative to natural processes: a case study in Narragansett Bay, Rhode Island. In: Benaka, L.R. (Ed.), Fish Habitat: Essential Fish Habitat and Rehabilitation. American Fisheries Society, Symposium 22, Bethesda, Maryland, pp. 224–237.

Dufau-Julliand, C., Marsaleix, P., Petrenko, A., Dekeyser, I., 2004. 3D modeling of the Gulf of Lion's hydrodynamics (NW Med.) during January 1999 (MOOGLI3 experiment) and late winter 1999: WIW formation and cascading over the shelf break. Journal of Geophysical Research 109, C11002.

Dufois, F., Garreau, P., Le Hir, P., Forget, P. Wave- and current-induced bottom shear stress distribution in the Gulf of Lions. Continental Shelf Research, this issue, doi:10.1016/j.csr.2008.03.028.

Durrieu de Madron, X., Nyffeler, F., Godet, C.H., 1990. Hydrographic structure and nepheloïd spatial distribution in the Gulf of Lions continental margin. Continental Shelf Research 10, 915–929.

Durrieu de Madron, X., Abassi, A., Heussner, S., Monaco, A., Aloisi, J.C., Radakovitch, O., Giresse, P., Buscail, R., Kerhervé, P., 2000. Particulate matter and organic carbon budgets for the Gulf of Lions (NW Mediterranean). Oceanologica Acta 23 (6), 717–730.

Durrieu de Madron, X., Denis, L., Diaz, F., Garcia, N., Guieu, C., Grenz, C., Loÿe-Pilot, M.D., Ludwig, W., Moutin, T., Raimbault, P., Ridame, C., 2003. Nutrients and carbon budgets for the Gulf of Lion during the Moogli cruises. Oceanologica Acta 26, 421–433.

Durrieu de Madron, X., Ferré, B., Le Corre, G., Grenz, C., Conan, P., Pujo-Pay, M., Bodiot, O., Buscail, R., 2005. Trawling-induced resuspension and dispersal of muddy sediments and dissolved elements. Continental Shelf Research 25 (19/20), 2387–2409.

Dyer, K.R., 1986. Coastal and Estuarine Sediment Dynamics. Wiley, London.

El Ganaoui, O., Schaaff, E., Boyer, P., Amielh, M., Anselmet, F., Grenz, C., 2004. The deposition and erosion of cohesive sediments determined by a multi-class model. Estuarine, Coastal and Shelf Science 60 (3), 457–475.

Estournel, C., Kondrachoff, V., Marsaleix, P., Vehil, R., 1997. The plume of the Rhône: numerical simulation and remote sensing. Continental Shelf Research 17, 899–924.

Estournel, C., Broche, P., Marsaleix, P., Devenon, J.L., Auclair, F., Vehil, R., 2001. The Rhone river plume in unsteady conditions: numerical and experimental results. Estuarine, Coastal and Shelf Science 53, 25–38.

Estournel, C., Durrieu de Madron, X., Marsaleix, P., Auclair, F., Julliand, C., Vehil, R., 2003. Observations and modelisation of the winter coastal oceanic circulation in the Gulf of Lions under wind conditions influenced by the continental orography (FETCH experiment). Journal of Geophysical Research 108 (C3), 8059.

Ferré, B., Guizien, K., Durrieu de Madron, X., Palanques, A., Guillén, J., Grémare, A., 2005. Fine sediment dynamics study during a winter storm in the Gulf of Lion shelf (NW Mediterranean), en révision à Continental Shelf Research. Continental Shelf Research 25 (19/20), 2410–2427.

Garcia-Estevez, J., 2005. Transferts géochimiques en Méditerranée: exemple de la rivière Têt et de son bassin versant. Ph.D. Thesis, University of Perpignan, p. 263.

Geernaert, G.L., 1990. Bulk parameterizations for the wind stress and heat fluxes. In: Geenaert, G.L., Plant, W.J. (Eds.), Surface Waves and Fluxes, vol. I—Current Theory. Kluwer Academic Publishers, p. 336.

Grant, W.D., Madsen, O.S., 1982. Movable bed roughness in unsteady oscillatory flow. Journal of Geophysical research 87, 469–481.

Guillén, J., Bourrin, F., Palanques, A., Durrieu de Madron, X., Puig, P., Buscail, R., 2006. Sediment dynamics during "wet" and "dry" storm events on the Têt inner shelf (SW Gulf of Lions). Marine Geology 234, 129–142.

Gust, G., Morris, M.J., 1989. Erosion thresholds and entrainment rates of undisturbed in situ sediments. Journal of Coastal Research 5, 87–99.

Harris, C.K., Wiberg, P.L., 2001. A two-dimensional, time-dependent model of suspended sediment transport and bed reworking for continental shelves. Computers and Geosciences (27), 675–690.

Heussner, S., Durrieu de Madron, X., Calafat, A., Canals, M., Carbonne, J., Delsaut, N., Saragoni, G., 2006. Spatial and temporal variability of downward particle fluxes on a continental slope: lessons from an 8-yr experiment in the Gulf of Lions (NW Mediterranean). Marine Geology 234, 63–92.

Hill, P.S., Syvitski, J.P., Cowan, E.A., Powell, R.D., 1998. Insitu observations of floc settling velocities in Glacier Bay, Alaska. Marine Geology 145, 85–94.

Houwing, E.J., 1999. Determination of the critical erosion threshold of cohesive sediments on intertidal mudflats along the Dutch Wadden sea coast. Estuarine, Coastal and Shelf Science 49, 545–555.

Houwing, E.J., 2000. Sediment dynamics in the pioneer zone in the land reclamation area of the Wadden Sea, Groningen, the Netherlands. Ph.D. Thesis, University of Utrecht, Utrecht.

Krishnappan, B.G., Marsalek, J., 2002. Transport characteristics of fine sediment from an on-stream stormwater management pond. Urban Water 4, 3–11.

Lapouyade, A., Durrieu de Madron, X., 2001. Seasonal variability of the advective transport of particulate matter and organic carbon in the Gulf of Lion (NW Mediterranean). Oceanologica Acta 24, 295–312.

Li, M.Z., Amos, C.L., 1998. Predicting ripple geometry and bed roughness under combined waves and currents in a continental shelf environment. Continental Shelf Research 18 (9), 941–970.

Li, M.Z., Amos, C.L., 2001. SEDTRANS96: the upgraded and better calibrated sediment-transport model for continental shelves. Computers and Geosciences (27), 619–645.

Maa, J.P., Sanford, L., Halka, J.P., 1998. Sediment resuspension characteristics in Baltimore Harbor, Maryland. Marine Geology 146, 137–145.

Marsaleix, P., Estournel, C., Kondrachoff, V., Vehil, R., 1998. A numerical study of the formation of the Rhone river plume. Journal of Marine Systems 14, 99–115.

Marsaleix, P., Auclair, F., Floor, J.W., Herrmann, M.J., Estournel, C., Pairaud, I., Ulses, C., 2008. Energy conservation issues in sigma-coordinate free-surface ocean models. Ocean Modelling 20, 61–89.

Meadows, P.S., Tait, J., Hussain, S.A., 1990. Effects of estuarine infauna on sediment stability and particle sedimentation. Hydrobiologia 190, 263–266.

Millot, C., 1999. Circulation in the western Mediterranean Sea. Journal of Marine Systems 20 (1–4), 423–442.

Monaco, A., Durrieu de Madron, X., Radakovitch, O., Heussner, S., Carbonne, J., 1999. Origin and variability of downward biogeochemical fluxes on the Rhône continental margin (NW Mediterranean). Deep-Sea Research I 46, 1483–1511.

Mulder, H.P., Udink, C., 1991. Modelling of cohesive sediment transport. A case study: the western Scheldt estuary. In: Edge, B.L. (Ed.), Proceedings of the 22nd International Conference on Coastal Engineering, ASCE, pp. 3012–3023.

Munk, W.H., Anderson, E.R., 1948. Notes on a theory of the thermocline. Journal of Marine Research 1, 276–295.

Nielsen, P., 1986. Suspended sediment concentrations under waves. Coastal Engineering 10, 23–31.

Oey, L.Y., Chen, P., 1992. A model simulation of circulation in the northeast Atlantic shelves and seas. Journal of Geophysical Research 97, 20,087–20,115.

Palanques, A., Puig, P., Guillén, J., Jiménez, J., Gracia, V., Sánchez-Arcilla, A., Madsen, O., 2002. Near-bottom suspended sediment fluxes on the microtidal low-energy Ebro continental shelf (NW Mediterranean). Continental Shelf Research 22, 285–303.

Palanques, A., Durrieu de Madron, X., Puig, P., Fabres, J., Guillén, J., Calafat, A., Canals, M., Heussner, S., Bonnin, J., 2006. Suspended sediment fluxes and transport processes in the Gulf of Lions submarine canyons. The role of storms and dense water cascading. Marine Geology 234, 43–61.

Panagiotopoulos, I., Voulgaris, G., Collins, M.B., 1997. The influence of clay on the threshold of movement on fine sandy beds. Coastal Engineering 32, 19–43.

Partheniades, E., 1962. A study of erosion and deposition of cohesive soils in salt water. Ph.D. Thesis, University of California, Berkeley, 182pp.

Pethelet-Giraud, E., Negrel, P.-H., Cubizolles, J., 2003. Flux exportés de l'Hérault vers la Méditerranée et origine des masses d'eau. Rapport BRGM /RP-52748-FR.

Petrenko, A., Leredde, Y., Marsaleix, P., 2004. Circulation in a stratified and wind-forced Gulf of Lions, NW Mediterranean Sea: in situ and modelling data. Continental Shelf Research 25 (1), 7–27.

Poirel, A., Carrel, G., Olivier, J.M., 2001. Illustration de la complémentarité des chroniques environnementales dans l'étude d'un hydrosystème fluvial: régime thermique et peuplements piscicoles du Rhône. In: Workshop "Activities in the Catchment Area and Water Quality," Lyon Fleuves 2001, Juin 2001.

Schaaff, E., Grenz, C., Pinazo, C., 2002. Erosion of particulate inorganic and organic matter in the Gulf of Lion. Comptes Rendus Géosciences 334, 1071–1077.

Sempéré, R., Charrière, B., Van Wambeke, F., Cauwet, G., 2000. Carbon inputs of the Rhone River to the Mediterranean Sea: biogeochemical implications. Global Biogeochemical Cycles 14, 669–681.

Serrat, P., 1999. Present sediment yield from a Mediterranean fluvial system: the Agly river (France). Comptes Rendus de l'Académie des Sciences—Series IIA—Earth and Planetary Science 329, 189–196.

Serrat, P., Ludwig, W., Navarro, B., Blazi, J.L., 2001. Spatial and temporal variability of sediment fluxes from a coastal Mediterranean river: the Têt (France). Comptes Rendus de l'Académie des Sciences—Series IIA—Earth and Planetary Science 333, 389–397.

Soulsby, R.L., Whithouse, R.J.S.W., 1997. Threshold of sediment motion in coastal environments. Proceedings of Pacific Coasts and Ports'97 Conference, Christchurch 1, 149–154.

Soulsby, R.L., Hamm, L., Klopman, G., Myrhaug, D., Simons, R.R., Thomas, G.P., 1993. Wave–current interaction within and outside the bottom boundary layer. Coastal Engineering 21, 41–69.

Torfs, H., 1995. Erosion of mud/sand mixtures. Ph.D. Thesis, Katholieke Universiteit Leuven, Faculteit der Toegepaste Wetenschappen, Departement Burgelijke Bouwkunde, Laboratorium voor Hydraulica.

Ulses, C., Estournel, C., Bonnin, J., Durrieu de Madron, X., Marsaleix, P., 2008. Impact of storms and dense water cascading on shelf–slope exchanges in the Gulf of Lion (NW Mediterranean). Journal of Geophysical Research 113, C02010, doi:10.1029/2006JC003795.

Ulses, C., Estournel, C., Durrieu de Madron, X., Palanques, A. Suspended sediment transport in the Gulf of Lion (NW Mediterranean): impact of extreme flood and storm. Continental Shelf Research, this issue, doi:10.1016/j.csr.2008.01.015.

Wentworth, C.K., 1922. A scale of grade and class terms for clastic sediments. Journal of Geology 30, 377–392.

Wheatcroft, R.A., 1994. Temporal variation on bed configuration and one-dimensional bottom roughness at the mid-shelf STRESS site. Continental Shelf research 14, 1167–1190.

Widdows, J., Brinsler, M.D., Bowley, N., Barrett, C., 1998. A benthic annular flume for in situ measurement of suspension feeding/biodeposition rates and erosion potential of intertidal cohesive sediments. Estuarine, Coastal and Shelf Sciences 46, 27–38.

Zanke, U., 1977. Berechnung der Sinkgeschwindichkeiten von Sedimenten. Mitteilungen des Franzius-Institutes 46, 231–245.

Zyserman, J.A., Fredsøe, J., 1994. Data analysis of bed concentration of suspended sediment. Journal of Hydraulic Engineering, ASCE 120 (9), 1021–1041.